EurJOC
European Journal of Organic Chemistry

A Journal of
ChemPubSoc Europe

Accepted Article

Title: Malonic Acid Derivatives on Duty as Electron-Withdrawing Units in Push-Pull Molecules

Authors: Milan Klikar, Veronika Jelínková, Zdeňka Růžičková, Tomáš Mikysek, Oldřich Pytela, Miroslav Ludwig, and Filip Bures

To be cited as: *Eur. J. Org. Chem.* 10.1002/ejoc.201700070

Link to VoR: http://dx.doi.org/10.1002/ejoc.201700070

Supported by
ACES Asian Chemical Editorial Society

WILEY-VCH

10.1002/ejoc.201700070

WILEY-VCH

FULL PAPER

Malonic Acid Derivatives on Duty as Electron-Withdrawing Units in Push-Pull Molecules

Milan Klikar,[a] Veronika Jelínková,[a] Zdeňka Růžičková,[b] Tomáš Mikysek,[c] Oldřich Pytela,[a] Miroslav Ludwig,[a] and Filip Bureš*[a]

Abstract: Based on the 2-(*N*-piperidinyl)thiophene central donor, 32 model push-pull molecules with systematically varied malonic acid-derived peripheral acceptors have been prepared. Further property tuning has been achieved by modifying the π-linker and the structural arrangement (linear vs. quadrupolar D-π-A systems). Malonic acid derivatives such as cyanoacetic acid, malondinitrile, diethyl malonate, Meldrum´s acid, and *N*,*N*´-dibutyl(thio)barbituric acid as well as 1,3-diketo analogues dimedone and indan-1,3-dione were employed as acceptor moieties. Knoevenagel condensation with four thiophene aldehydes afforded target chromophores in satisfactory yields. Withdrawing abilities of malonic acid acceptors were examined both by experiment including X-ray analysis, differential scanning calorimetry, electrochemistry, and UV-Vis absorption spectroscopy and by DFT calculations. Thorough structure-property relationships have been elucidated. According the increasing electron withdrawing ability, the widely used malonic acid acceptor units can be ordered as follows: diethyl malonate ≤ cyanoacetic acid < malondinitrile < Meldrum's acid < dimedone ≤ *N*,*N*'-dibutylbarbituric acid < indan-1,3-dione ≤ *N*,*N*'-dibutylthiobarbituric acid.

Introduction

Malonic acid (MA) was prepared for the first time by oxidation of malic acid by French chemist V. Dessaignes already in 1858.[1] Since this early experiment, malonic acid and its derivatives became well-known and widely studied class of organic compounds. They are extensively used in industry, especially in pharmaceuticals, agrochemicals, vitamins, dyes, adhesives, and fragrances.[2] A common feature of MA derivatives is high reactivity of the central methylene bridge. Due to acidity of the CH_2, induced by two neighboring carbonyl groups, these compounds easily undergo alkylation, arylation, aldol and Knoevenagel condensations, and MA derivatives are also often utilized in the construction of heterocycles.[3] Knoevenagel condensation is one of the main synthetic tools used for introducing MA derivatives into the structure of push-pull chromophores. This reaction between a carbonyl compound and a substance bearing active methylene group is generally acid- or base-catalyzed.[4]

Organic push-pull chromophores currently constitute intensively investigated class of π-conjugated systems, which has found many applications across chemistry and material sciences.[5] The unique and peculiar properties of push-pull molecules such as color, (hyper)polarizability, dipolar character, and extraordinary linear and nonlinear optical behavior, etc. are mainly induced by intramolecular charge transfer (ICT) from the electron donor via π-linker to the electron acceptor.[6] Optical properties, HOMO-LUMO gap, dipole moments, hyperpolarizabilty coefficients, etc. are mainly dictated by the extent of the ICT. In push-pull molecules, the aforementioned fundamental properties can easily be tuned by the type of used electron donors and acceptors, length and composition of the π-linker, and overall chromophore arrangement.[7] High importance of D-π-A systems can clearly be demonstrated by their wide applications as active substances in organic electronics, molecular optics,[8] and semiconductors.[9] For many decades, MA derivatives have widely been used as electron withdrawing parts of push-pull chromophores. Their popularity can be ascribed to their commercial availability, low price, easy incorporation into the chromophore, and relatively high electron withdrawing character. Moreover, a right choice of MA derivative enables facile fine-tuning of target chromophore properties. According to the functional groups, MA derivatives can be divided into three general subgroups: i) *nitriles* (e.g. cyanoacetic acid, ethyl cyanoacetate, and malondinitrile, ii) *esters* (e.g. dialkyl malonate and Meldrum´s acid), and iii) *imides* (e.g. (thio)barbituric acid).

Malonic acid and cyanoacetic acid are currently privileged precursors for the construction of chromophores for DSSC (dye-sensitized solar cell).[10] The principal advantage of cyanoacetic acid can be seen in combining both withdrawing (-CN) and anchoring (-COOH) abilities. Malondinitrile,[11] as a starting compound for the formation of dicyanovinyl (DCV) withdrawing unit, is one of the most popular electron acceptor ever. For instance, DCV unit has extensively been studied by Diederich et al.[12] and recently reviewed by us.[13] More recently, we have prepared a series of model tripodal molecules with peripheral cyano acceptors including DCV moiety. This study clearly demonstrates a strong withdrawing ability of DCV unit compared to other used cyano acceptors.[14] On the contrary, dialkyl malonates have rarely been employed in the construction of push-pull chromophores.[15] It is probably due to its weak withdrawing ability caused by +M effects of alkoxy groups. Meldrum´s acid as a cyclic ester of malonic acid is likewise scarcely used in push-pull chromophores, but it was used in some D-π-A systems so

[a] Institute of Organic Chemistry and Technology, Faculty of Chemical Technology, University of Pardubice, Studentská 573, Pardubice, 53210, Czech Republic.
E-mail: filip.bures@upce.cz; Web: http://bures.upce.cz
Fax: +420 46 603 7068; Tel: +420 46 603 7099
[b] Department of General and Inorganic Chemistry, Faculty of Chemical Technology, University of Pardubice, Studentská 573, Pardubice 53210, Czech Republic.
[c] Department of Analytical Chemistry, Faculty of Chemical Technology, University of Pardubice, Studentská 573, Pardubice 53210, Czech Republic.

Supporting information for this article is given via a link at the end of the document.

far.[16] On the other hand, barbituric acid and its thio analogue are very popular MA derivatives with noticeable withdrawing strength. These acceptor moieties abundantly occurs in many (mero)cyanine dyes,[17] nonlinear optic chromophores,[18] solvatochromic[19] and near-infrared probes[20] dyes for DSSCs,[21] and supramolecular complexes based on multiple H-bonding interactions.[22] In 2013, we have utilized *N*,*N*´-dibutylbarbituric acid as powerful and well-soluble acceptor moiety of push-pull chromophores with systematically elongated π-linker.[23] Recently, we have also focused on multipodal push-pull molecules end-capped with DCV or *N*,*N*´-dibutylbarbituric unit(s).[24] This preceding research inspired us to study and critically compare withdrawing abilities of acceptor units based on various MA derivatives. It is quite surprising that, to the best of our knowledge, no attempts have been made to systematically compare withdrawing strength of wide range of malonic derivatives. Beside pure MA derivatives, this study also involves two additional 1,3-diketo analogues such as dimedone and indan-1,3-dione. Whereas dimedone, representing an analogue of Meldrum´s acid, was used very scarcely in organic (opto)electronics,[25] indan-1,3-dione proved to be a very powerful acceptor, for instance in our recent T-shaped chromophores.[26] The electron withdrawing abilities of the particular MA-derivatives can roughly be estimated according to their pK_a values.

The withdrawing strength of the particular acceptors as well as influence of the branching and extension of the π-linker were investigated by electrochemistry, UV/Vis absorption spectra, DSC, X-ray analysis, and DFT quantum chemical calculations. Based on the measured and calculated data, structure-property relationships have been elucidated and discussed.

Results and Discussion

In overall, we have designed and prepared 32 push-pull chromophores (31 new) bearing eight electron acceptor parts as well as extended and branched π-conjugated system based on 2-(*N*-piperidinyl)thiophene (PIT) donor/linker (Figure 1). As precursors of the particular MA derivative were utilized: cyanoacetic acid (CAA), malondinitrile (MDN), diethyl malonate (DEM), Meldrum´s acid (MEL), *N*,*N*´-dibutylbarbituric acid (DBB), *N*,*N*´-dibutyl-2-thiobarbituric acid (DBTB), dimedone (DMD), and indan-1,3-dione (IND).

According to structural features, all target chromophores **1**-**8** can be divided in four subseries **a**-**d**. The chromophore number specifies type of the acceptor(s): **1** = CAA, **2** = MDN, **3** = DEM, **4** = MEL, **5** = DMD, **6** = DBB, **7** = DBTB, and **8** = IND. Labels **a**-**d** indicates length of the π-linker (ethenylene in series **a** and **c**; but-1,3-dienylene in series **b** and **d**) as well as degree of branching (linear **a** and **b**; branched **c** and **d**).

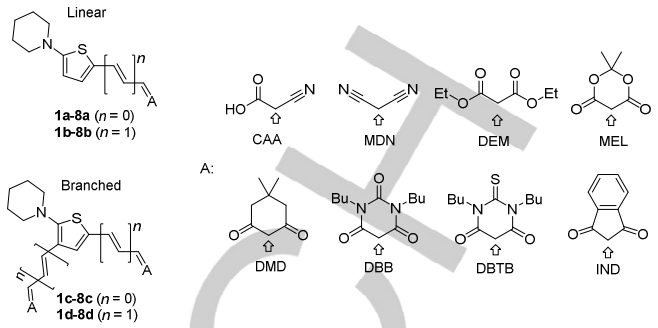

Figure 1. Target linear/branched chromophores with eight withdrawing units based on MA derivatives and its analogues.

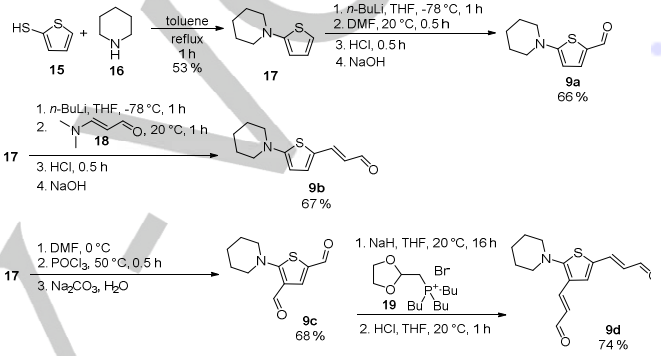

Scheme 1. Construction of PIT aldehydes **9a**-**d**.

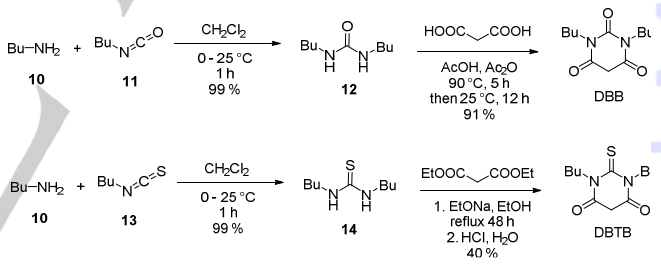

Scheme 2. Synthesis of *N*,*N*´-dibutyl(thio)barbituric acids DBB and DBTB.

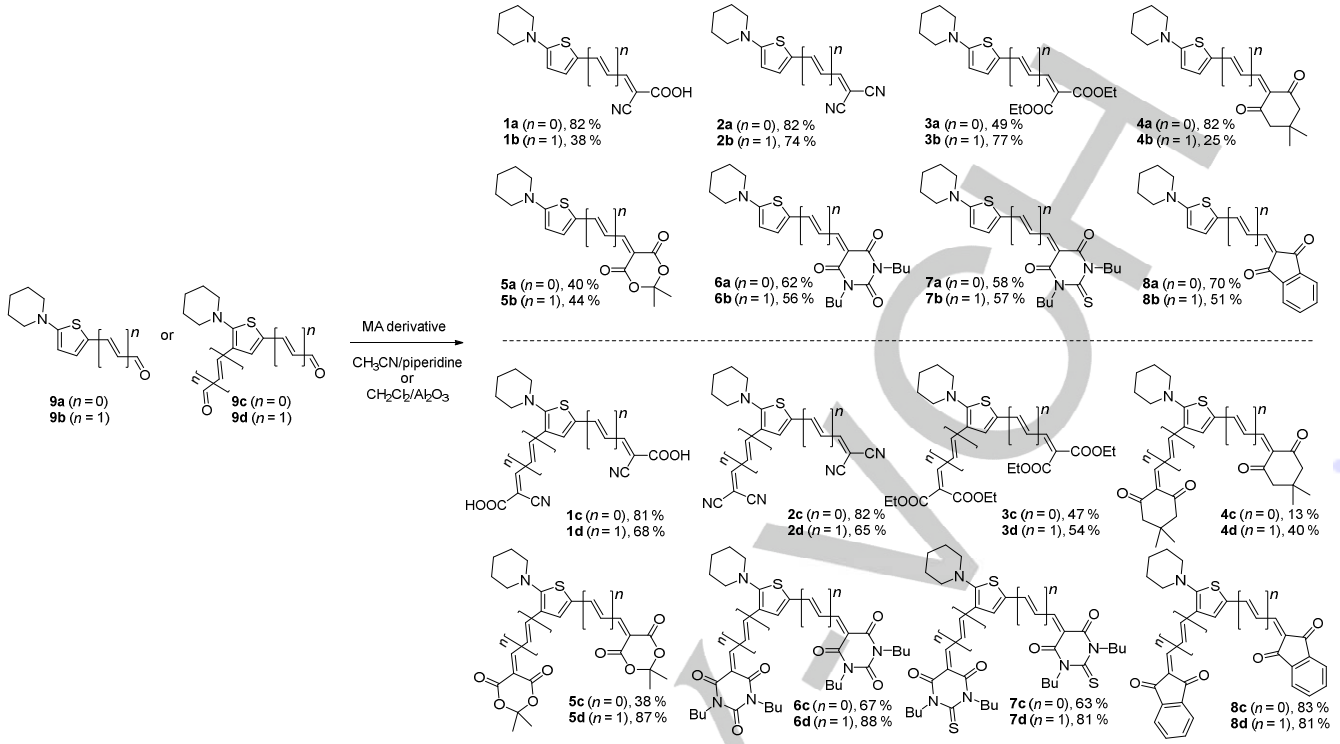

Scheme 3. General synthetic pathway towards chromophores **1**-**8** via Knoevenagel condensation.

Synthesis

In general, all target push-pull chromophores **1**-**8** were prepared via Knoevenagel condensation. Cyanoacetic acid (CAA), malondinitrile (MDN), diethyl malonate (DEM), Meldrum´s acid (MEL), dimedone (DMD), and indan-1,3-dione (IND) are commercially available. The remaining acceptor precursors, namely *N*,*N*´-dibutylbarbituric acid (DBB) and *N*,*N*´-dibutyl-2-thiobarbituric acid (DBTB) were synthesized via acid/base catalyzed condensation of *N*,*N*´-dibutyl(thio)ureas **12** and **14** with malonic acid or diethyl malonate according to Scheme 1. Detailed synthetic procedures are given in the SI.

Scheme 2 shows overall preparations of PIT aldehydes. PIT (**17**), as a fundamental D/π building block, was prepared by the reaction of thiophene-2-thiol **15** with piperidine **16** with 53% yield.[27] Its direct lithiation with *n*-BuLi at -78 °C and subsequent reaction with DMF afforded linear aldehyde **9a** with 66% yield.[28] A similar reaction sequence with 3-(*N*,*N*-dimethylamino)acrolein **18** afforded extended aldehyde **9b** with 67% yield. PIT also underwent Vilsmeier-Haack formylation with DMF/$POCl_3$ system.[29] In contrast to available reports, [28,29] we have isolated only dialdehyde **9c** regardless of the used amount of DMF/$POCl_3$. This twofold formylation provided branched dialdehyde **9c** in satisfactory yield of 68 %. However, all attempts to perform similar Vilsmeier-Haack formylation of **17** with **18** resulted in very exothermic reaction and decomposition. Hence, extended dialdehyde **9d** was prepared via alternative twofold Wittig elongation of **9c** using commercially available phosphonium salt **19**.[28] Subsequent hydrolysis of the formed diacetal intermediate yielded **9d** with 74% yield. Detailed synthetic procedures and characterization (including X-rays) of all four aldehydes **9a**-**d** are given in the SI.

With PIT aldehydes **9a**-**d** in hand, we have carried out their Knoevenagel condensations with aforementioned MA derivatives (Scheme 3). As the particular MA derivatives exhibit various basicity/nucleophilicity and aldehydes **9a**-**d** possess different reactivity/electrophilicity, the reaction conditions had to be optimized. In some reactions, a generally well-working and very convenient CH_2Cl_2/Al_2O_3 system[30,23,12-14] had to be replaced by CH_3CN/piperidine one. The Knoevenagel reactions of **9a**-**d** with parent MA provided completly insoluble compounds. The particular reaction conditions are listed in the Experimental section. The attained yields do not show any noticeable trends, they rather represent an intersection of acid-base properties of the starting materials as well as the used separation techniques.

X-ray analysis

Crystals of PIT aldehydes **9a**-**d** as well as target chromophores **2c**, **4a**, **5b**, and **8a**-**b** suitable for X-ray analysis were obtained by slow diffusion of hexane into its dichloromethane solution. The ORTEP plots of PIT aldehydes are shown in Figure S1 in the SI, for target chromophores see Figure 2. These plots confirm the proposed molecular structures as well as arrangement of the particular aldehyde/chromophore in the solid state. The ORTEP plot of **9c** further confirms observed twofold Vilsmeier-Haack formylation taking place selectively at the C3 and C5 positions of the PIT.

The MA-derived acceptor units in **2c**, **4a**, **5b**, and **8a**-**b** are almost perfectly co-planar with the central thiophene moiety. Regardless of the used π-linker (ethenylene or but-1,3-dienylene),

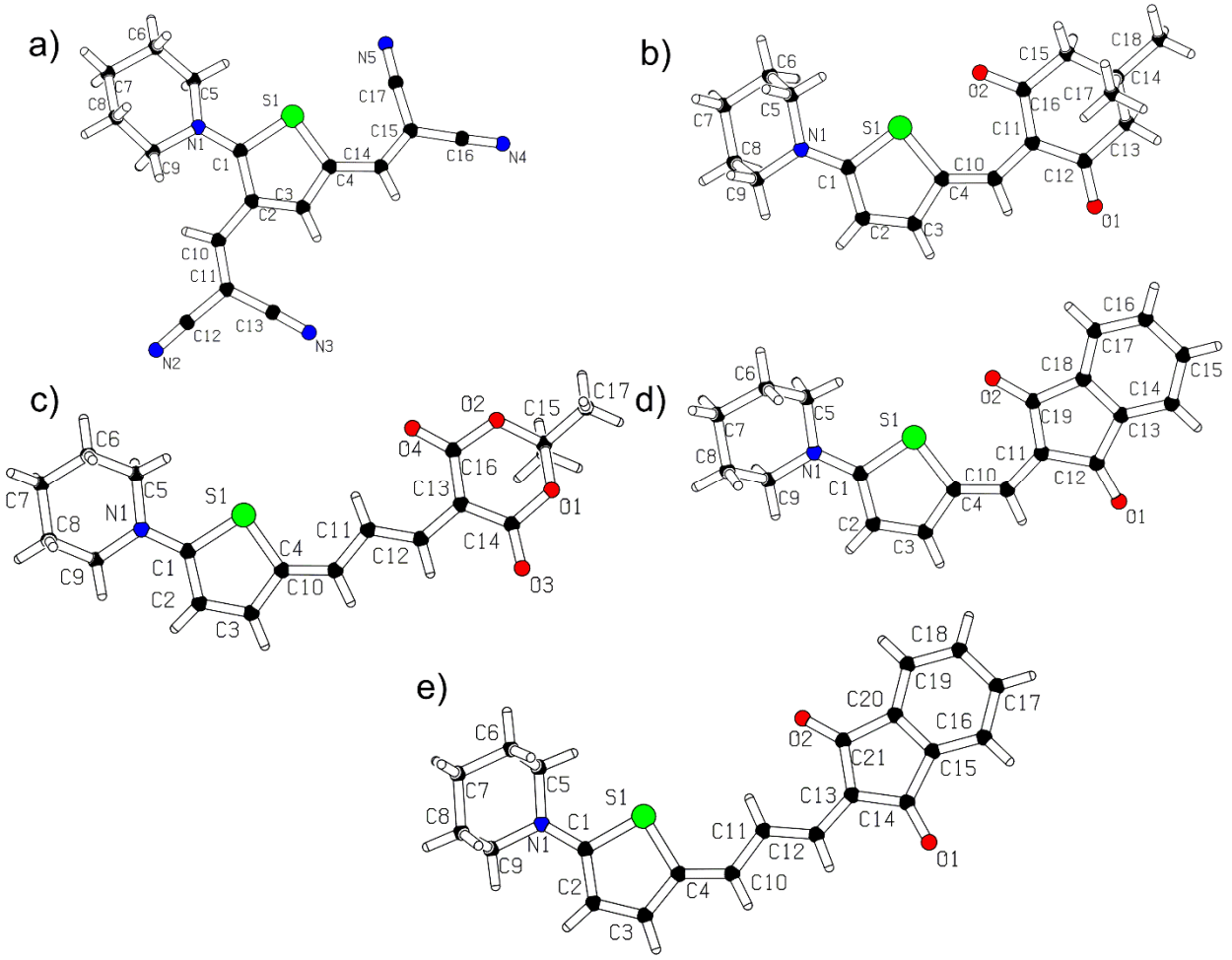

Figure 2. X-ray molecular representations of chromophores **2c** (a), **4a** (b), **5b** (c), **8a** (d), and **8b** (e).

the dihedral angles between these two moieties do not exceed 10 ° (generally 1-3 °). This allows efficient overlap of the π-electron clouds across the whole π-system and facilitates the ICT between the donor and the acceptor. Branching of the chromophore caused only minor deviation of the piperidine ring.

A variation of the C-C bond distances within the thiophene ring in a range from typical C=C double bond to ca 1.42 Å has been revealed from the X-ray data. This can be attributed to elongated thiophene bonds, while the rest of the C–C, C–N and C–O (multiple) bonds are localized at appropriate places with lengths similar to the literature values. In this respect, the extent of the ICT can be assessed by calculating bond length alternation within the central thiophene ring. Its quinoid character/aromaticity can easily be determined by the Bird index I_5).[31] Whereas the Bird index of unsubstituted thiophene equals to 66, thiophene rings in **2c**, **4a**, **5b**, and **8a**-**b** possess I_5 within the range of 59 to 63. This implies less aromaticity and higher quinoid character of the thiophene rings due to the ICT. However, the PIT donor connected to a powerful T-shaped, indan-1,3-dione-derived acceptor can be polarized even further with I_5 = 58.[26b]

The supramolecular arrangement of **2c**, **4a**, **5b**, and **8a**-**b** reveals 2D-layered array structures due to extensive π-π stacking supported by numerous non-covalent C-H···negative atom interactions.

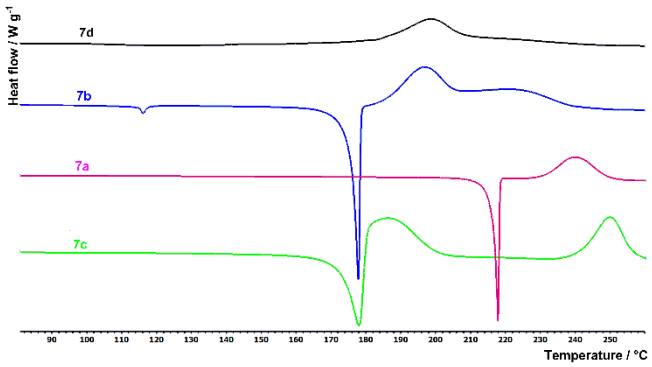

Figure 3. Representative DSC curves of compounds **7a**-**d** (DBTB chromophores) determined with a scanning rate of 3 °C/min under N_2.

Thermal properties

Thermal behaviour of compounds **1**-**8** was studied by differential scanning calorimetry (DSC). Figure 3 shows thermograms of representative compounds **7a**-**d** (DBTB chromophores) while Table 1 lists all measured melting points (T_m) and temperatures of thermal decompositions (T_d). All DCS curves are given in the SI. The measured melting points range from 62 to 261 °C. The temperature of decomposition was estimated within the range of 171-303 °C.

Except **1a**, all linear chromophores in series **a** exhibited very sharp endothermic peak of melting. Chromophore **3a** is viscous oil, which decomposed directly at 269 °C followed by a melting of the decomposed residue. For **4a** and **7a**, the exothermic peaks of decomposition were observed shortly after melting, while **1a**, **2a**, **5a**, **6a**, and **8a** were stable in liquid phase for additional 40-150 °C above their melting point. Except **3b** bearing DEM acceptor unit (T_m = 62 °C), very sharp peaks of melting were found for compounds in series **b** (T_m = 155-213 °C). In contrast to **1b**-**3b**, and **6b**, decomposition of **4b**, **5b**, **7b**, and **8b** followed immediately their melting.

The compounds in branched series **c** and **d** showed complex thermal behaviour. Compounds **2c** and **6c** exhibited sharp melting peaks followed by gradual decomposition, while the melting of **4c**, **5c**, **7c**, and **8c** was immediately overset to exothermic decompositions. For most compounds in series **c** the subsequent decomposition peaks were observed as well. Oily **3c** exhibited similar thermal behavior as **3a**. Whereas **2d** and **5d** decomposed immediately after melting, **6d** and especially **3d** were stable also in liquid phase. On the contrary, compounds **1d**, **4d**, **7d**, and **8d** decomposed directly without melting.

Desorption of the residual/crystalline solvents were observed for compounds **1b**, **1c**, **1d**, **5b**, **6d**, and **8d**. Moreover, **5c** and **6d** also showed solid-solid transitions at 125 and 140 °C, respectively.

From the measured thermal properties, we can conclude the following outcomes:

- Elongation of the π-linker by embedding an additional double bond decreases T_d (e.g. linear series **b** vs. **a**; Figure 3).
- The measured T_d values are very close (ΔT_d = 5-40 °C) for pairs of compounds with the same acceptors in series **c** and **d** (Figure 3).
- In general, the linear compounds **1a**-**8a** and **1b**-**8b** always showed melting peaks, whereas the branched **1c**-**8c** and **1d**-**8d** often underwent additional thermal processes or decomposed directly without melting.
- The lowest melting points were determined for **3b** (62 °C) and **3d** (123 °C) with DEM acceptor bearing ethyl chains. In general, alkyl chains hamper crystallization and significantly affect the melting points.
- On the contrary, compounds end-capped with DEM unit(s) (**3a**-**d**) exhibited the highest average T_d values.
- Similarly, CAA-, MDN-, and IND-terminated compounds (**1a**-**d**, **2a**-**d**, and **8a**-**d**) significantly resisted thermal decomposition.
- MEL-substituted **5a**-**d** possess higher T_d compared to structurally similar DMD **4a**-**d** (effect of the oxygen atoms).
- The effect of chalcogenide atom can be distinguish between DBB (**6a**-**d**) and DBTB (**7a**-**d**) derivatives. The sulfur atom in DBTB increases the melting point and generally decreases T_d compared to DBB oxygen analogs.

With respect to the aforementioned conclusions, the highest melting point and decomposition temperature were observed for **2d** (T_d = 261 °C) and **2a** (T_d = 303 °C) end-capped with MDN acceptor unit(s).

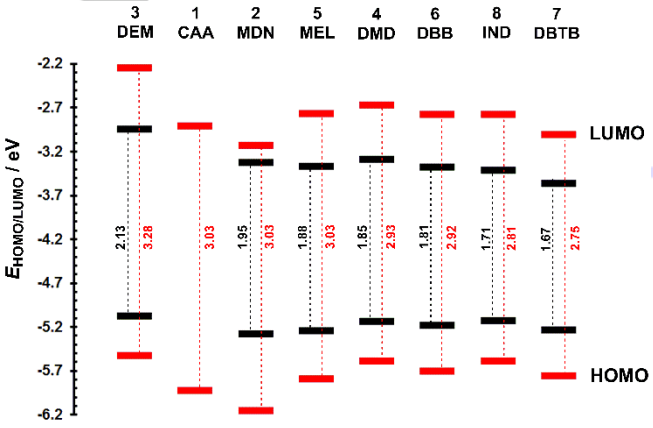

Figure 4. Energy level diagram of averaged values of the electrochemical (black) and DFT calculated (red) energies $E_{HOMO/LUMO}$ for the particular series of MA-derived withdrawing units.

Electrochemistry

Electrochemical measurements of chromophores **1**-**8** were carried out in *N*,*N*-dimethylformamide containing 0.1 M Bu_4NPF_6 in a three electrode cell by cyclic voltammetry (CV) and rotating disk voltammetry (RDV). The working electrode was glassy carbon disk (2 mm in diameter) for CV and RDV experiments. As reference and auxiliary electrodes were used saturated calomel electrode (SCE) separated by a bridge filled with supporting

10.1002/ejoc.201700070

electrolyte and Pt wire, respectively. All potentials are given *vs.* SCE. Table 1 lists the acquired data, representative CV diagrams of compounds **2c**, **3d**, **4a**, **5b**, **6c**, **7d**, and **8a** are given in the SI. Chromophores **1a**-**d** with CAA acceptor(s) were not measurable by the employed electrochemical techniques.

The values of the half-wave potentials of the first oxidation and reduction $E_{1/2(ox1)}$ and $E_{1/2(red1)}$ were recorded within the range of 0.53 to 1.15 and -1.63 to -0.52 V, respectively. The first oxidation and reduction are typical one-electron processes, followed by subsequent oxidations and reductions, and are obviously a function of the number and type of the used acceptor unit(s) as well as the π-linker length (Table 1). Whereas the first oxidation most likely takes place at the PIT donor, the first reduction is situated on the withdrawing moiety and the adjacent π-linker. All half-wave potentials of the first oxidation and reduction were further recalculated to the energies of the HOMO and LUMO ($E_{HOMO/LUMO}$), respectively.[32] Hence, the further discussion will be given in terms of these quantities and their differences ΔE as these fit better purposes of this article. Energy level diagram of averaged values of the $E_{HOMO/LUMO}$ for the given quartet of chromophores with the same acceptor unit is shown in Figure 4.

As a general trend, the E_{HOMO} values gradually decreased in order **b** → **d** → **a** → **c**. Hence, extension of the π-linker shifts the HOMO levels to more positive values most significantly (**b** vs. **a** or **d** vs. **c**). Chromophore branching has the opposite effect and further reduces the E_{HOMO} values (**c** vs. **a** or **d** vs. **b**). The lowest/highest averaged HOMO level belong to chromophores **2**/**3** bearing MDN/DEM acceptor units.

On average, the E_{LUMO} values decreased in order **a** → **b** → **c** → **d**. In contrast to the HOMO levels, the E_{LUMO} is shifted to more negative values both upon extension of the π-system and branching the chromophore. Hence, the lowest/highest averaged E_{LUMO} values were measured for chromophore **7**/**3** with DBTB/DEM acceptor units. As the first reduction and the LUMO are localized on the acceptor moieties of **1**-**8**, the energies E_{LUMO} can be used to order the particular acceptor units as follows: DEM < DMD ≤ MDN ≤ MEL ≤ DBB < IND < DBTB.

Table 1. Summarized thermal, electrochemical, and linear optical properties of chromophores **1**-**8**.

Compound	T_m [a] (°C)	T_d [b] (°C)	$E_{1/2(ox1)}$ [c] (V)	$E_{1/2(red1)}$ [c] (V)	ΔE [c] (V)	E_{HOMO} [e] (eV)	E_{LUMO} [e] (eV)	λ_{max}^A [f] (nm/eV)	$\varepsilon_{max}^A \cdot 10^3$ ($M^{-1} \cdot cm^{-1}$)
1a	130	205	- [g]	- [g]	-	-	-	436/2.84, 459/2.70[h]	28.8/45.9[h]
2a	143	303	0.95[d]	-1.29	2.24	-5.30	-3.06	464/2.67	57.9
3a	-	269	0.72	-1.63	2.35	-5.07	-2.72	430/2.88	36.1
4a	205	217	0.83	-1.36	2.19	-5.18	-2.99	488/2.54	81.4
5a	184	232	0.94[d]	-1.30[d]	2.24	-5.29	-3.05	468/2.65	90.5
6a	172	251	0.88[d]	-1.28[d]	2.16	-5.23	-3.07	486/2.55	110.6
7a	216	231	0.94[d]	-1.15[d]	2.09	-5.29	-3.20	508/2.44	120.8
8a	182	243	0.80	-1.21[d]	2.01	-5.15	-3.14	515/2.41	105.1
1b	155	217	- [g]	- [g]	-	-	-	468/2.65, 533/2.33[h]	17.5/23.7[h]
2b	155	254	0.67	-1.02	1.69	-5.02	-3.33	551/2.25	73.3
3b	62	258	0.53	-1.33	1.86	-4.88	-3.02	466/2.66	35.2
4b	169	179	0.59	-1.03	1.62	-4.94	-3.32	594/2.09	109.8
5b	213	218	0.67	-0.96	1.63	-5.02	-3.39	572/2.17	142.1
6b	148	207	0.64	-0.95	1.59	-4.99	-3.40	592/2.09	142.1
7b	175	186	0.69	-0.82	1.51	-5.04	-3.53	614/2.02	174.9
8b	204	215	0.56[d]	-0.93	1.49	-4.91	-3.42	619/2.00	123.0
1c	-	264	- [g]	- [g]	-	-	-	398/3.12, 448/2.77[h]	14.7/14.1[h]
2c	215	222	1.24	-0.92	2.16	-5.59	-3.43	472/2.63	30.3
3c	-	298	0.96[d]	-1.45[d]	2.41	-5.31	-2.90	386/3.21	28.3
4c	204	209	0.97	-1.02	1.99	-5.32	-3.33	497/2.49	42.7
5c	199	205	1.15[d]	-0.90[d]	2.05	-5.50	-3.45	477/2.60	41.1
6c	127	171	1.04[d]	-0.90	1.94	-5.39	-3.45	527/2.35	39.4
7c	172	179	1.09[d]	-0.65	1.74	-5.44	-3.70	519/2.39	87.9
8c	243	254	1.00	-0.85	1.85	-5.35	-3.50	556/2.23	48.3
1d	-	250	- [g]	- [g]	-	-	-	433/2.86, 465/2.67[h]	17.8/19.1[h]
2d	261	264	0.85	-0.85	1.70	-5.20	-3.50	522/2.38	36.8
3d	123	286	0.71	-1.21	1.92	-5.06	-3.14	423/2.93	37.1
4d	-	214	0.76	-0.85	1.61	-5.11	-3.50	583/2.13	29.2
5d	235	244	0.85	-0.75	1.60	-5.20	-3.60	579/2.14	47.8
6d	178	212	0.79	-0.75	1.54	-5.14	-3.60	598/2.07	54.8
7d	-	184	0.85	-0.52	1.37	-5.20	-3.83	656/1.89	68.0
8d	-	242	0.75	-0.74	1.49	-5.10	-3.61	585/2.12	43.2

[a] T_m = melting point (the point of intersection of a baseline and a tangent of thermal effect = oneset). [b] T_d = thermal decomposition (pyrolysis in N_2 atmosphere). [c] $E_{1/2(ox1)}$ and $E_{1/2(red1)}$ are half-wave potentials of the first oxidation and reduction, respectively; all potentials are given vs. SCE; $\Delta E = E_{1/2(ox1)} - E_{1/2(red1)}$. [d] Reversible process. [e] $-E_{HOMO/LUMO} = E_{1/2(ox1/red1)} + 4.429$ (Ref.[32]). [f] Measured in CH_3OH/CH_2Cl_2 24:1 at concentration 10^{-5} M. [g] Not measurable. [h] 5 µl of AcOH were added to measured solutions.

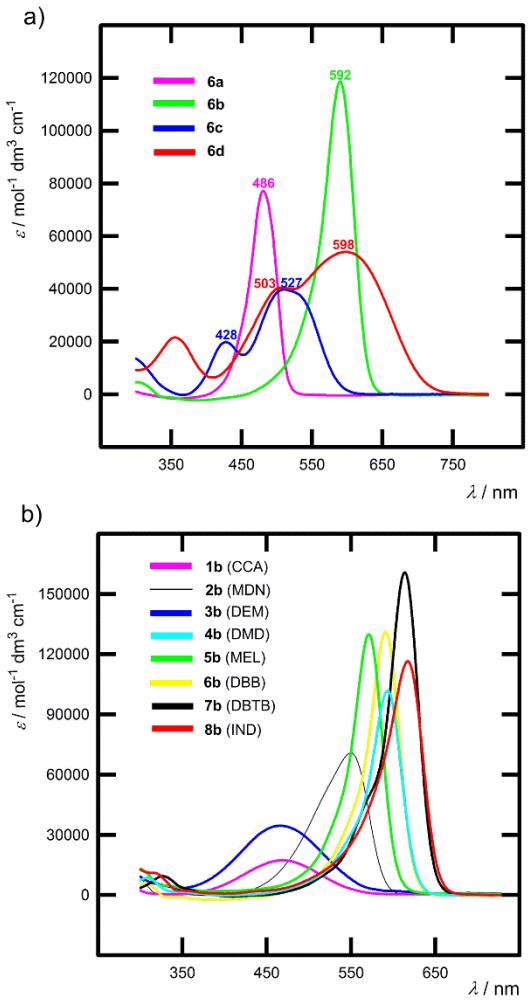

Figure 5. Representative, mathematically smoothed (Ref.[33]) UV-Vis absorption spectra of DBB chromophores **6a-d** (a) and **1b-8d** in CH_3OH/CH_2Cl_2 (24:1) at concentration 1×10^{-5} M.

The difference between the first oxidation and reduction potentials/HOMO and LUMO levels (electrochemical gap, ΔE) represents a direct way for evaluating the extent of the ICT across all withdrawing units and chromophores. As the electron donating part (PIT) remained unaltered in all chromophores, the changes seen in the $E_{HOMO/LUMO}$ can be ascribed to the following structural changes:

- Length of the π-linker. Its extension always reduces the ΔE.
- Chromophore branching reduces the ΔE as well. This effect is especially pronounced when going from linear series **a** to branched series **c** and less for series **b** and **d** in which the effect of the π-linker elongation dominates.
- The HOMO-LUMO gap in **1-8** is mostly dictated by the withdrawing unit appended to the PIT donor. According to decreasing ΔE values, we can order the acceptor units as follows: DEM < MDN < MEL ≤ DMD < DBB < IND < DBTB (Figure 4).

Hence, chromophores **7d** (1.37 eV), **8b**, and **8d** (both 1.49 eV) bearing DBTB and IND acceptor units possess the narrowest ΔE. On the contrary, DEM-terminated molecules **3a** (2.35 eV) and **3c** (2.41 eV) possess the largest HOMO-LUMO gaps.

One photon absorption

All target chromophores **1-8** are intensely colored solids or oils with a color ranging from yellow to blue (see Figure S10 in the SI), most of them showed none emissive properties. Hence, optical absorption properties were examined by UV-Vis spectroscopy. The longest-wavelength absorption maxima λ_{max} and molar absorption coefficients ε_{max} are summarized in Table 1. Selected absorption spectra are shown in Figure 5, for complete listing see the SI. The longest-wavelength absorption maxima of chromophores **1-8** ranged from 386 to 656 nm with the corresponding ε_{max} values of 15 to 175 × 10^3 $M^{-1}\cdot cm^{-1}$.

Linear chromophores in series **a** and **b** exhibit always a single CT-band, whereas the spectra of branched molecules in series **c** and **d** feature two more or less developed CT-bands (Figure 5a). This reflects two conjugated pathways between both particular acceptors and the PIT central donor and their quadrupolar nature. According to the Frenkel exciton model, the excited state of a quadrupolar molecule is split to two bands which are energetically positioned at +V and -V (V is the inter-branch coupling) relative to the excited state of the parent dipolar molecule.[34] For quadrupolar branched molecules are both bands one-photon allowed (observable), while the low-energy lying one possesses greater oscillator strength (larger ε_{max}). This is also the case of chromophores **6a**/**6c** and **6b**/**6d** (Figure 5a). For instance, **6a** possesses one single CT-band with λ_{max} = 486 nm and ε_{max} = 110.6 × 10^3 $M^{-1}\cdot cm^{-1}$, while the spectrum of its quadrupolar analogue **6c** features two bands at 428 and 527 nm with ε_{max} = 24.3 and 39.4 × 10^3 $M^{-1}\cdot cm^{-1}$, respectively. Figure 5a also clearly demonstrates the effect of π-linker elongation. When going from **6a** to **6b** or from **6c** to **6d** (insertion of one double bond in each branch), the positions of the longest-absorption maxima shifted bathochromically with $\Delta\lambda_{max}$ of 106 and 71 nm, respectively.

The trends seen by electrochemical measurements are also obeyed in electronic absorption spectra. Namely, extension of the

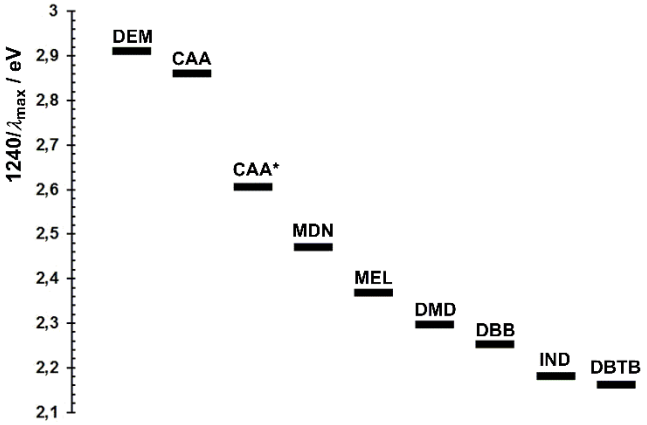

Figure 6. Comparison of averaged optical gaps ($1240/\lambda_{max}$) for the particular series of MA-derived withdrawing units. * Acetic acid was added.

π-linker of the chromophore reduces the optical gap (1240/λ_{max}), see Table 1. Chromophore branching has no clear trends across the whole series as two peaks for quadrupolar chromophores in series **c** and **d** were observed. Hence, both red- and slight blue-shifts were observed (Table 1). Alternation of the acceptor units affects the optical properties of chromophores **1**-**8** most significantly. For instance, a gradual replacement of the DEM acceptor in **3b** (λ_{max} = 466 nm) up to DBTB or IND shifted the λ_{max} to 614 (**7b**) and 619 (**8b**) nm, respectively ($\Delta\lambda_{max}$ ~ 150 nm, Figure 5b). Thus, a right choice of the MA acceptor allows tuning of the optical gap by about 0.7 eV. Figure 6 compares the averaged optical gaps of all MA derivatives. Considering the λ_{max}-derived optical gaps, the withdrawing abilities of the particular MA derivatives showed the same trend as seen by ΔE values (see their correlation in Figure S55) with the following order: DEM ≤ CAA < MDN < MEL < DMD ≤ DBB < IND ≤ DBTB.

The following structure-withdrawing property relationships can be deduced among the particular MA-acceptors:

- DEM is the weakest electron acceptor, DBTB and IND are the most powerful ones.
- MDN proved to be stronger acceptor unit than CAA.
- The withdrawing behavior of CAA strongly depends on the extent of the COOH dissociation. Acidification of the media by acetic acid (Figure 6), resulted in significant red-shift of the spectra as the COOH remained undissociated.
- Cyclic MEL proved to be much stronger acceptor than linear DEM (lactone vs. ester). Hence, cyclic MA-derivatives are generally stronger electron acceptors.
- O→C replacement in MEL lead to DMD (ester vs. ketone) with improved withdrawing ability (counterproductive saturation of the carbonyls by alkoxy groups in MEL).
- Chalcogenide O→S replacement as in DBB vs. DBTB significantly affects properties of both acceptors. The latter proved much stronger.
- O→N replacements as in CAA vs. MDN or MEL vs. DBB enhances the withdrawing power and, therefore, MDN and DBB are stronger acceptors than CAA and MEL, respectively.
- When comparing 1,3-diketones DMD and IND, the latter showed much stronger withdrawing ability as a result of the fused benzene ring allowing enlarged conjugation.

Quantum chemical calculations

Spatial and electronic properties of all target chromophores **1**-**8** were investigated at the DFT level using Gaussian W09 package.[35] The geometries of molecules **1**-**8** were optimized by DFT B3LYP/6-311++G(2d,p) method. Energies of the HOMO and LUMO, their differences, ground state dipole moments μ and first hyperpolarizabilities β were also calculated on the DFT B3LYP/6-311++G(2d,p) level. All calculated data are summarized in Table 2.

The calculated energies of the HOMO and LUMO of **1**-**8** range from -6.69 to -5.27 and from -3.57 to -1.92 eV, respectively. They are obviously a function of the branching, extension of the π-linker, and type of the attached acceptor moiety. The calculated HOMO-LUMO gaps (ΔE^{DFT}) are generally a bit wider than those obtained by electrochemistry, however the trends within the whole series of molecules are clearly preserved (Figure 4). Moreover, the calculated HOMO-LUMO differences correlate tightly with both electrochemical and optical gaps (Figure S56-S57) and, therefore, the used DFT method can be considered as a reasonable tool describing electronic properties of **1**-**8**. For instance, the narrowest ΔE^{DFT} of 2.47 eV was calculated for chromophore **7d** with DBTB acceptor moiety, similarly to the electrochemical outcome. In general, the averaged ΔE^{DFT} values of **1**-**8** decrease in the order of DEM > CAA ≈ MDN ≈ MEL > DMD ≈ DBB > IND > DBTB, which resembles the order deduced from the electrochemical and optical properties.

The HOMO and LUMO localizations in representative chromophores **5b** and **8d** are shown in Figure 7. Complete listing is given in the SI. Molecules in linear series **a** and **b**, e.g. **5b**, possess the HOMO and the HOMO-1 localized predominantly on the piperidinyl donor and partially in the alternating positions. The LUMO is spread over the MEL acceptor part, adjacent π-linker, and partially also on the piperidinyl residue. The LUMO+1 is localized on the thiophene central part. Branched chromophores in series **c** and **d**, e.g. **8d**, showed very similar localization of the HOMO and HOMO-1, whereas the LUMO is spread mostly over the IND acceptor appended on the remote branch. The second branch closer to the piperidinyl donor is occupied by the LUMO+1. This distribution of the LUMO orbitals is a common feature of branched push-pull molecules.[14,34] Surprisingly, chromophores **7a**-**d** have the HOMO localized on the sulphur and oxygen atoms of the DBTB acceptor.

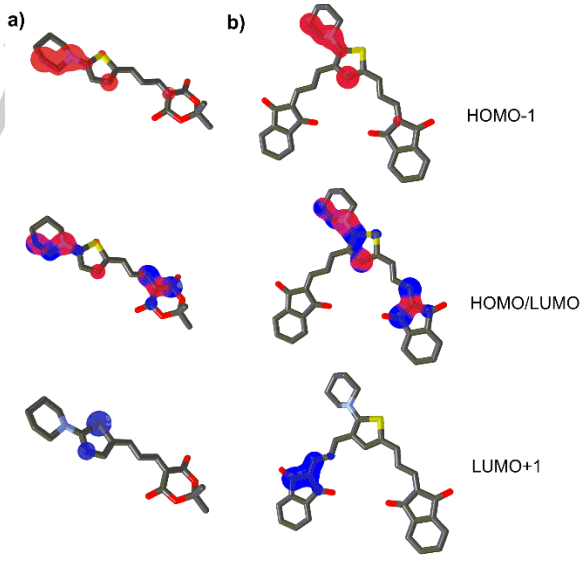

Figure 7. HOMO/HOMO-1 (red) and LUMO/LUMO+1 (blue) localizations in **5b** (a) and **8d** (b).

Table 2. DFT calculated parameters of chromophores **1**-**8**.

Compound	E_{HOMO} [a] (eV)	E_{LUMO} [a] (eV)	ΔE^{DFT} (eV)	μ [a] (D)	$\beta \times 10^{-30}$ [a] (esu)	Compound	E_{HOMO} [a] (eV)	E_{LUMO} [a] (eV)	ΔE^{DFT} (eV)	μ [a] (D)	$\beta \times 10^{-30}$ [a] (esu)
1a	-5.75	-2.46	3.29	10.9	34	**1c**	-6.40	-3.14	3.26	12.5	47
2a	-5,89	-2.67	3.22	12.8	38	**2c**	-6.69	-3.41	3.28	9.4	43
3a	-5.39	-1.92	3.47	7.1	52	**3c**	-5.73	-2.08	3.65	2.3	53
4a	-5.54	-2.31	3.23	6.8	57	**4c**	-5.86	-2.74	3.12	3.4	92
5a	-5.71	-2.39	3.32	8.3	41	**5c**	-6.17	-2.89	3.28	5.1	67
6a	-5.65	-2.41	3.24	9.2	51	**6c**	-5.99	-2.89	3.10	5.9	86
7a	-5.69	-2.63	3.06	10.9	30	**7c**	-6.05	-3.19	2.86	6.9	370
8a	-5.52	-2.47	3.05	6.9	134	**8c**	-5.76	-2.89	2.87	4.7	295
1b	-5.57	-2.76	2.81	15.4	194	**1d**	-5.99	-3.29	2.70	14.9	659
2b	-5.66	-2.88	2.78	15.1	182	**2d**	-6.39	-3.57	2.82	8.7	304
3b	-5.27	-2.25	3.02	10.4	198	**3d**	-5.74	-2.73	3.01	7.8	288
4b	-5.34	-2.61	2.73	8.6	319	**4d**	-5.60	-3.00	2.60	5.5	3343
5b	-5.48	-2.68	2.80	10.2	233	**5d**	-5.82	-3.13	2.69	7.0	906
6b	-5.44	-2.70	2.74	11.1	299	**6d**	-5.74	-3.12	2.62	9.0	2316
7b	-5.49	-2.88	2.61	13.1	368	**7d**	-5.82	-3.35	2.47	11.3	829
8b	-5.34	-2.69	2.65	8.5	707	**8d**	-5.74	-3.08	2.66	4.0	28222[b]

[a] Calculated at the DFT B3LYP/6-311++G(2d,p) level; [b] Most likely overestimated value (repeated calculations always with the same result).

The calculated ground state dipole moments range from 2.3 to 15.4 D. In general, the highest values were calculated for chromophores with CAA (**1a**-**d**), MDN (**2a**-**d**), and DBTB (**7a**-**d**) acceptors (9-15 D). On the contrary, chromophores with diketo acceptors such as DMD (**4a**-**d**) and IND (**8a**-**d**) showed significantly diminished μ values (2-8 D). Extension of the π-linker generally increased the dipole moment, while branching has rather opposite effect.

Polarizabilities of the chromophores **1**-**8** have also been evaluated by calculating the first hyperpolarizabilities β (Table 2). Excluding **8d** as an outlier, the calculated β values range from 30 to 3343 × 10^{-30} esu. Compared to linear chromophores **1a**-**8a** (β = 30-134 × 10^{-30} esu), extension of the π-linker as in **1b**-**8b** resulted in significant improvement of the first hyperpolarizability β up to 182-707 × 10^{-30} esu. Similar and even pronounced trend can be seen when comparing series **c** and **d**. Branched chromophores in series **c** and **d** possess up to one order of magnitude higher β values than the corresponding linear analogues in series **a** and **b**. From the MA-derived acceptor moieties, the DBTB and IND impart the strongest ICT into the molecule, which also reflects their generally highest calculated NLO coefficients in series **a**-**c**. However, in the branched and most extended series **d**, the highest β values were calculated for **4d**, **6d**, (and **8d**) bearing 1,3-diketo (DMD and IND) or DBB acceptors. Hence, indan-1,3-dione and (thio)barbituric acids seems to be the most powerful acceptors from the whole series of push-pull molecules.

Conclusions

In order to study withdrawing ability of six malonic acid derivatives and two its analogues, new model push-pull chromophores have been designed and synthesized. First, a straightforward reaction path towards four PIT aldehydes has been developed. These aldehydes underwent smooth Knoevenagel condensation with eight different MA-derivatives to afford 32 mostly new push-pull molecules **1**-**8** in four series **a**-**d**. These chromophores have systematically varied peripheral acceptor moiety, structural arrangement, and length of the π-linker. Thorough structure-property relationships have been elucidated considering both experimental (thermal, electrochemical, and optical) and calculated data.

Molecular structures of all PIT aldehydes **9a**-**d** as well as five target chromophores **2c**, **4a**, **5b**, and **8a**-**b** were confirmed by X-ray analysis, which revealed considerably planar structures, high quinoid character of the central thiophene ring, and extensive π-π stacking in the solid state.

DSC analysis showed that π-linker extension decreased thermal robustness, branching mostly caused direct decomposition without melting, and variation of the peripheral withdrawing moiety affected thermal property of **1**-**8** according to its nature. Hence, the highest thermal robustness has been observed for MDN-terminated molecules as well as for CAA-, DEM-, and IND-derivatives.

The electrochemical and UV/Vis absorption optical measurements revealed the same trends and structural features influencing the fundamental properties of target chromophores **1**-**8**. Namely, the π-linker extension and gradual chromophore branching reduces both electrochemical and optical gaps. However, the HOMO/LUMO levels and resulting gaps are predominantly dictated by the composition, electronic, and spatial nature of the used acceptor. A replacement of the particular atoms (O→C, O→N, and O→S) within the acceptor unit significantly improves its electron withdrawing ability. Cyclic acceptors proved to be stronger than linear analogues. Extended π-conjugation (e.g. IND) further enhances withdrawing behavior.

The aforementioned conclusion are further fully supported by the performed DFT calculations. The calculated data correlates tightly with the electrochemical and optical properties.

Hence, based on the experimental as well as calculated properties, the particular MA-derived acceptors can be ordered as follows:

DEM ≤ CAA < MDN < MEL < DMD ≤ DBB < IND ≤ DBTB.

In general, the MA-derived acceptors can be classified in four subgroups:

- weak (DEM),
- moderate (CAA, MDN),
- powerful (MEL, DMD, DBB),
- and very strong (IND, DBTB).

The main goal of this work was to investigate and critically compare the withdrawing ability of the most used MA-derived acceptors. Therefore, a wide range of target MA-chromophores has been synthesized based on the PIT donor, which allowed proper evaluation of averaged experimental and theoretical results. We believe that the deduced outcomes may serve as a useful guide to conveniently select a proper MA-derivative for the given D-π-A system with desired optoelectronic behavior.

Experimental Section

General methods

The preparation and characterization of *N*,*N*´-dibutyl(2-thio)barbituric acids, PIT **17**, and aldehydes **9a-d** are given in the SI. The remaining acceptor precursors (CAA, MDN, DEM, MEL, DMD, IND) as well as starting compounds **10**, **11**, **13**, **15**, **16**, **18**, and **19** are commercially available. All commercial chemicals, reagents and solvents were purchased from Sigma Aldrich, Acros and TCI and were used as received. THF was dried in Puresolv™ micro solvent purification system. Lithiation and Wittig reaction were carried out in a flame-dried flasks under argon. Column chromatography was carried out with silica gel 60 (particle size 0.040-0.063 mm, 230-400 mesh; Merck) and commercially available solvents. Thin-layer chromatography (TLC) was conducted on aluminum sheets coated with silica gel 60 F254, obtained from Merck, with visualization by a UV lamp (254 or 360 nm). Thermal properties were measured by differential scanning calorimetry DSC with a Mettler-Toledo STARe System DSC 2/700 equipped with FRS 6 ceramic sensor and cooling system HUBERT TC100-MT RC 23. Thermal behavior of the target chromophores were measured in open aluminous crucibles under N_2 inert atmosphere. DSC curves were determined with a scanning rate of 3 °C/min within the range 25-450 °C. Melting point and temperature of decomposition were determined as intersection of the baseline and tangent of the peak (onset point). Elemental analyses were carried on a Fison EA 1108 instrument. ^{1}H and ^{13}C NMR spectra were recorded at 400 and 100 MHz, respectively, with a Bruker AVANCE 400 instrument or 500 and 125 MHz, respectively, with a Bruker Ascend™ 500 at 25 °C. Chemical shifts are reported in ppm relative to the signal of Me_4Si. The residual solvent signal in the ^{1}H and ^{13}C NMR spectra was used as an internal reference ($CDCl_3$ 7.25 and 77.23 ppm; CD_2Cl_2 5.32 and 54.00; DMSO-d_6 2.55 and 39.51; D_2O 4.80). Apparent resonance multiplicities are described as s (singlet), d (doublet), dd (doublet of doublet), t (triplet), q (quartet) and m (multiplet), apparent coupling constants of multiplets (^3J or ^4J) are given in Hz. Thiophene and aromatic indan-1,3-dione signals were marked as th and ind, respectively. IR spectra were recorded as neat using HATR adapter on a Perkin-Elmer FTIR Spectrum BX spectrometer. Mass spectra were measured with a GC-MS configuration comprised of an Agilent Technologies 6890N gas chromatograph equipped with a 5973 Network MS detector (EI 70 eV, mass range 33–550 Da). High resolution MALDI MS spectra were measured on a MALDI mass spectrometer LTQ Orbitrap XL (Thermo Fisher Scientific, Bremen, Germany) equipped with nitrogen UV laser (337 nm, 60 Hz). The LTQ Orbitrap instrument was operated in positive-ion mode over a normal mass range (*m/z* 50-2000) with resolution 100 000 at *m/z* = 400. The survey crystal positioning system (survey CPS) was set for the random choice of shot position by automatic crystal recognition. 2,5-Dihydroxybenzoic acid (DHB), 2-[(*E*)-3-(4-*tert*-butylphenyl)-2-methylprop-2-enylidene]propanedinitrile (DCTB) and 9-aminoacridine (9-AA) were used as a matrix. Mass spectra were averaged over the whole MS record for all measured samples. The absorption spectra were measured on a Hewlett–Packard 8453 spectrophotometer in CH_3OH/CH_2Cl_2 24:1 at concentration of 1×10^{-5} M. Voltammetric measurements were performed using a potentiostat PGSTAT 128N (AUTOLAB, Metrohm Autolab B.V., Utrecht, The Netherlands) operated via NOVA 1.11 software.

General Method for Knoevenagel condensation of 9a-d with cyanoacetic acid (i)

Aldehyde **9a**-**b** (1 mmol) and cyanoacetic acid (1.5 mmol) or dialdehyde **9c**-**d** (1 mmol) and cyanoacetic acid (3 mmol), were dissolved in CH_3CN (10 mL) and piperidine (0.5 mL; 5 mmol) was added dropwise. The reaction mixture was refluxed for 90 min, the solvents were removed *in vacuo* and the residue was dissolved in CH_2Cl_2 (20 mL). Acetic acid (about 1 mL) was added dropwise and the reaction mixture was stirred at 25 °C for 30 min. The solvent was partially evaporated *in vacuo* and the residue was purified by column or flash chromatography and then recrystallized from CH_2Cl_2/CH_3OH.

General Method for Knoevenagel condensation catalyzed by Al_2O_3 (ii)

Aldehyde **9a**-**b** (1 mmol) and acceptor precursor (1.2 mmol) or dialdehyde **9c**-**d** (1 mmol) and acceptor precursor (2.5 mmol), were dissolved in CH_2Cl_2 (25 mL) and Al_2O_3 (5 or 10 mmol, Brockmann II-III) were added. The reaction mixture was stirred at 25 °C for 18 hours. The reaction

mixture was filtered and the solvent was evaporated *in vacuo*. The crude product was purified by column chromatography.

General Method for Knoevenagel condensation catalyzed by piperidine (iii)

Aldehyde **9a**-**b** (1 mmol) and acceptor precursor (1.2 mmol) or dialdehyde **9c**-**d** (1 mmol) and acceptor precursor (2.5 mmol), were dissolved in CH_3CN (25 mL) and a few drops of piperidine were added. The reaction mixture was refluxed for 18 hours. The solvents were removed *in vacuo* and the crude product was purified by column chromatography.

Chromophore 1a. The title compound was synthesized from aldehyde **9a** (195 mg) following the general method (i). Yield: 215 mg (82 %); terracotta solid. R_f = 0.6 (SiO_2; CH_2Cl_2/CH_3OH 10:1); mp 130 °C. ^{1}H NMR (500 MHz, DMSO-d_6, 25 °C): δ = 1.66 (s, 6H, CH_2), 3.50-3.51 (m, 4H, CH_2), 6.50 (d, J = 4.5 Hz, 1H, CHth), 7.79 (d, J = 4.5 Hz, 1H, CHth), 8.12 ppm (s, 1H, CH). ^{13}C NMR (125 MHz, DMSO-d_6, 25 °C): δ = 23.11, 24.69, 50.75, 104.58, 119.47, 119.84, 141.89, 144.06, 166.39, 166.64 ppm. FT-IR (HATR): ν = 2920, 2852, 2359, 2201, 1648, 1571, 1496, 1402, 1238, 1197, 1174, 1132, 1099, 1012, 888, 758, 661 cm^{-1}. HR-MALDI-MS (9-AA): calcd for $C_{13}H_{13}N_2O_2S$ [M-H]$^+$ 261.06922; found 261.07157.

Chromophore 1b. The title compound was synthesized from aldehyde **9b** (221 mg) following the general method (i). Yield: 110 mg (38 %); red-black solid. R_f = 0.6 (SiO_2; CH_2Cl_2/CH_3OH 10:1); mp 155 °C. ^{1}H NMR (500 MHz, DMSO-d_6, 25 °C): δ = 1.60-1.65 (m, 6H, CH_2), 3.30-3.32 (m, 4H, CH_2), 6.19 (d, J = 4 Hz, 1H, CHth), 6.33 (dd, J_1 = 12 Hz, J_2 = 15 Hz, 1H, CH), 7.13 (d, J = 4 Hz, 1H, CHth), 7.31 (d, J = 14.5 Hz, 1H, CH), 7.70 ppm (d, J = 12 Hz, 1H, CH). ^{13}C NMR (125 MHz, DMSO-d_6, 25 °C): δ = 23.18, 24.59, 50.79, 69.81, 104.48, 116.19, 118.79, 124.42, 134.53, 137.55, 150.28, 162.21, 165.83 ppm. FT-IR (HATR): ν = 2834, 2361, 2210, 1584, 1441, 1312, 1223, 1146, 1074, 964, 888, 763 cm^{-1}. HR-MALDI-MS (DCTB): calcd for $C_{15}H_{17}N_2O_2S$ [M+H]$^+$ 289.10052; found 289.17153.

Chromophore 1c. The title compound was synthesized from dialdehyde **9c** (223 mg) following the general method (i). Yield: 290 mg (81 %); dark orange solid. R_f = 0.9 (SiO_2; CH_2Cl_2/CH_3OH 1:1). ^{1}H NMR (400 MHz, D_2O, 25 °C): δ = 1.65-1.74 (m, 6H, CH_2), 3.36-3.38 (m, 4H, CH_2), 7.86 (s, 1H, CH), 7.90 (s, 1H, CH), 7.96 ppm (s, 1H, CH). ^{13}C NMR (125 MHz, D_2O, 25 °C): δ = 22.99, 25.14, 55.96, 99.36, 102.94, 115.30, 119.17, 119.66, 122.06, 137.44, 143.72, 145.03, 169.16, 169.36, 171.17 ppm. FT-IR (HATR): ν = 3404, 2210, 1603, 1444, 1357, 1338, 1288, 1183, 789 cm^{-1}. HR-MALDI-MS (9-AA): calcd for $C_{17}H_{14}N_3O_4S$ [M-H]$^+$ 356.06995; found 356.07267.

Chromophore 1d. The title compound was synthesized from dialdehyde **9d** (276 mg) following the general method (i). Yield: 278 mg (68 %); red-brown solid. R_f = 0.9 (SiO_2; CH_3OH). ^{1}H NMR (400 MHz, DMSO-d_6, 25 °C): δ = 1.53-1.54 (m, 2H, CH_2), 1.70 (s, 4H, CH_2), 3.00-3.03 (m, 4H, CH_2), 6.51 (dd, J_1 = 11.6 Hz, J_2 = 14.8 Hz, 1H, CH), 6.84 (dd, J_1 = 11.6 Hz, J_2 = 15.2 Hz, 1H, CH), 6.97 (d, J = 15.2 Hz, 1H, CH), 7.26 (d, J = 14.8 Hz, 1H, CH), 7.39 (s, 1H, CHth), 7.57 (d, J = 11.6 Hz, 1H, CH), 7.65 ppm (d, J = 11.6 Hz, 1H, CH). ^{13}C NMR not measurable due to a low solubility of **1d** in common deuterated solvents. FT-IR (HATR): ν = 2359, 2215, 1594, 1365, 1298, 1154, 980, 789 cm^{-1}. HR-MALDI-MS (DCTB): calcd for $C_{21}H_{19}N_3O_4S$ [M]$^+$ 409.10908; found 409.11051.

Chromophore 2a. The title compound was synthesized from aldehyde **9a** (195 mg) and malondinitrile (79 mg) following the general method (ii). Yield: 200 mg (82 %); orange solid. R_f = 0.75 (SiO_2; CH_2Cl_2); mp 143 °C. Found: C, 64.09; H, 5.43; N, 17.19; S, 12.94; $C_{13}H_{13}N_3S$ requires C, 64.17; H, 5.39; N, 17.27; S, 13.18 %. ^{1}H NMR (500 MHz, $CDCl_3$, 25 °C): δ = 1.68-1.75 (m, 6H, CH_2), 3.46-3.48 (m, 4H, CH_2), 6.13 (d, J = 4.5 Hz, 1H, CHth), 7.33 (s, 1H, CHth), 7.39 ppm (s, 1H, CH). ^{13}C NMR (125 MHz, CD_2Cl_2, 25 °C): δ = 23.84, 25.62, 52.06, 105.88, 116.97, 117.75, 119.68, 145.68, 148.72, 170.75 ppm. FT-IR (HATR): ν = 2918, 2190, 1575, 1513, 1487, 1446, 1402, 1266, 1078, 769 cm^{-1}. HR-MALDI-MS (DHB): calcd for $C_{13}H_{13}N_3S$ [M]$^+$ 243.08247; found 243.08273.

Chromophore 2b. The title compound was synthesized from aldehyde **9b** (222 mg) and malondinitrile (80 mg) following the general method (ii). Yield: 200 mg (74 %); violet solid. R_f = 0.7 (SiO_2; CH_2Cl_2); mp 155 °C. Found: C, 66.82; H, 5.70; N, 15.59; S, 11.79; $C_{15}H_{15}N_3S$ requires C, 66.88; H, 5.61; N, 15.60; S, 11.90 %. ^{1}H NMR (500 MHz, $CDCl_3$, 25 °C): δ = 1.66-1.75 (m, 6H, CH_2), 3.39-3.41 (m, 4H, CH_2), 6.07 (d, J = 4.5 Hz, 1H, CHth), 6.42 (dd, J_1 = 12 Hz, J_2 = 14 Hz, 1H, CH), 7.16-7.19 (m, 2H, CHth+CH), 7.29 ppm (d, J = 12 Hz, 1H, CH). ^{13}C NMR (125 MHz, $CDCl_3$, 25 °C): δ = 23.67, 25.20, 51.53, 106.02, 114.32, 114.46, 116.48, 123.81, 140.28, 143.36, 159.02, 167.42 ppm. FT-IR (HATR): ν = 2919, 2852, 2189, 1578, 1514, 1421, 1326, 1218, 1166, 1127, 1058, 963 cm^{-1}. HR-MALDI-MS (DHB): calcd for $C_{15}H_{15}N_3S$ [M]$^+$ 269.09812; found 269.09854.

Chromophore 2c. The title compound was synthesized from dialdehyde **9c** (222 mg) and malondinitrile (165 mg) following the general method (ii). Yield: 261 mg (82 %); burgundy red solid. R_f = 0.8 (SiO_2; EtOAc/Hex 1:1); mp 215 °C. Found: C, 63.70; H, 4.15; N, 21.89; S, 9.87; $C_{17}H_{13}N_5S$ requires C, 63.93; H, 4.10; N, 21.93; S, 10.04 %. ^{1}H NMR (500 MHz, $CDCl_3$ 25 °C): δ = 1.77-1.79 (m, 2H, CH_2), 1.83-1.86 (m, 4H, CH_2), 3.55-3.57 (m, 4H, CH_2), 7.48 (s, 1H, CH), 7.65 (s, 1H, CH), 8.08 ppm (s, 1H, CH). ^{13}C NMR (125 MHz, $CDCl_3$, 25 °C): δ = 23.35, 25.67, 57.04, 113.51, 113.75, 114.35, 114.45, 114.91, 122.61, 139.60, 149.05, 150.31, 173.92 ppm. FT-IR (HATR): ν = 2923, 2208, 1538, 1502, 1442, 1350, 1225, 1198, 853 cm^{-1}. HR-MALDI-MS (DHB): calcd for $C_{17}H_{13}N_5S$ [M]$^+$ 319.08862; found 319.08904.

Chromophore 2d. The title compound was synthesized from dialdehyde **9d** (276 mg) and malondinitrile (165 mg) following the general method (ii). After column chromatography, the product was refluxed with hexane (20 mL). The precipitate was filtered off, washed with EtOAc (10 mL), and dried Chromophore **2d** is sparingly soluble in common chlorinated solvents. Yield: 242 mg (65 %); black solid. R_f = 0.8 (SiO_2; CH_2Cl_2); mp 261 °C. Found: C, 66.92; H, 4.47; N, 18.89; S, 8.04; $C_{21}H_{17}N_5S$ requires C, 67.90; H, 4.61; N, 18.85; S, 8.63 %. ^{1}H NMR (500 MHz, CD_2Cl_2, 25 °C): δ = 1.70-1.80 (m, 6H, CH_2), 3.35-3.36 (m, 4H, CH_2), 6.70 (dd, J_1 = 12 Hz, J_2 = 15 Hz, 1H, CH), 6.90 (dd, J_1 = 11.5 Hz, J_2 = 15 Hz, 1H, CH), 7.13 (d, J = 15 Hz, 1H, CH), 7.26 (d, J = 14.5 Hz, 1H, CH), 7.42 (s, 1H, CHth), 7.50 (d, J = 12 Hz, 1H, CH), 7.55 ppm (d, J = 12 Hz, 1H, CH). ^{13}C NMR (125 MHz, CD_2Cl_2, 25 °C): δ = 23.94, 25.95, 56.39, 79.22, 79.63, 113.07, 114.92, 115.00, 119.75, 120.59, 121.58, 128.00, 134.92, 141.47, 142.28, 159.57, 160.77, 170.12 ppm. FT-IR (HATR): ν = 2352, 2205, 1559, 1475, 1345, 1217, 1153, 975 cm^{-1}. HR-MALDI-MS (DHB): calcd for $C_{21}H_{17}N_5S$ [M]$^+$ 371.11992; found 371.12018.

Chromophore 3a. The title compound was synthesized from aldehyde **9a** (195 mg) and diethyl malonate (192 mg) following the general method (iii). Yield: 165 mg (49 %); yellow-orange viscous oil. R_f = 0.6 (SiO_2; Hex/EtOAc 2:1). Found: C, 60.52; H, 7.00; N, 4.20; S, 9.49; $C_{17}H_{23}NO_4S$ requires C, 60.51; H, 6.87; N, 4.15; S, 9.50 %. ^{1}H NMR (400 MHz, $CDCl_3$, 25 °C): δ = 1.29 (t, J = 9 Hz, 3H, CH_3), 1.36 (t, J = 9 Hz, 3H, CH_3), 1.61-1.71 (m, 6H, CH_2), 3.28-3.31 (m, 4H, CH_2), 4.23 (q, J = 9 Hz, 2H, CH_2), 4.34 (q, J = 9 Hz, 2H, CH_2), 5.99 (d, J = 5.5 Hz, 1H, CHth), 7.18 (d, J = 5.5 Hz, 1H, CHth), 7.77 ppm (s, 1H, CH). ^{13}C NMR (125 MHz, $CDCl_3$, 25 °C): δ = 14.38, 14.54, 23.81, 25.19, 51.18, 60.98, 61.36, 103.89, 111.80, 120.42, 139.48, 141.20, 166.23, 167.15, 167.57 ppm. FT-IR (HATR): ν = 2936, 2855, 1694, 1589, 1514, 1441, 1376, 1239, 1055, 887, 856, 756 cm^{-1}. HR-MALDI-MS (DHB): calcd for $C_{17}H_{24}NO_4S$ [M+H]$^+$ 338.14206; found 338.14377.

10.1002/ejoc.201700070

Chromophore 3b. Aldehyde **9b** (221 mg) and diethyl malonate (160 mg) were dissolved in CH_3CN (25 mL), Al_2O_3 (510 mg; 5 mmol) and a few drops of piperidine were added. The reaction mixture was refluxed for 4 h, subsequently stirred at 25 °C for 16 h, filtered, and the solvent was evaporated *in vacuo*. The crude product was purified by column chromatography (SiO_2, CH_2Cl_2/acetone 100:5). Yield: 280 mg (77 %); dark red solid. R_f = 0.9 (SiO_2; CH_2Cl_2/acetone 100:5); mp 62 °C. Found: C, 62.74; H, 7.11; N, 3.82; S, 8.71; $C_{19}H_{25}NO_4S$ requires C, 62.78; H, 6.93; N, 3.85; S, 8.82 %. ^{1}H NMR (500 MHz, $CDCl_3$, 25 °C): δ = 1.29 (t, J = 7 Hz, 3H, CH_3), 1.36 (t, J = 7 Hz, 3H, CH_3), 1.59-1.62 (m, 2H, CH_2), 1.67-1.71 (m, 4H, CH_2), 3.23-3.25 (m, 4H, CH_2), 4.23 (q, J = 7 Hz, 2H, CH_2), 4.32 (q, J = 7 Hz, 2H, CH_2), 5.93 (d, J = 4 Hz, 1H, CHth), 6.74 (dd, J_1 = 12 Hz, J_2 = 15 Hz, 1H, CH), 6.92 (d, J = 4 Hz, 1H, CHth), 7.03 (d, J = 14.5 Hz, 1H, CH), 7.50 ppm (d, J = 12 Hz, 1H, CH). ^{13}C NMR (125 MHz, $CDCl_3$, 25 °C): δ = 14.47, 14.53, 23.81, 25.16, 51.43, 61.01, 61.04, 104.24, 117.25, 118.93, 125.91, 133.86, 139.59, 148.01, 163.29, 165.79, 166.21 ppm. FT-IR (HATR): ν = 2920, 2850, 2368, 1690, 1577, 1522, 1436, 1314, 1204, 1137, 1049, 1027, 749 cm^{-1}. HR-MALDI-MS (DHB): calcd for $C_{19}H_{26}NO_4S$ $[M+H]^+$ 364.15771; found 364.15930.

Chromophore 3c. The title compound was synthesized from dialdehyde **9c** (222 mg) and diethyl malonate (192 mg) following the general method (iii). Yield: 238 mg (47 %); yellow-brown viscous oil. R_f = 0.8 (SiO_2; CH_2Cl_2/EtOAc 20:1). Found: C, 59.27; H, 6.70; N, 2.61; S, 6.12; $C_{25}H_{33}NO_8S$ requires C, 59.15; H, 6.55; N, 2.76; S, 6.32 %. ^{1}H NMR (500 MHz, $CDCl_3$, 25 °C): δ = 1.25-1.34 (m, 12H, CH_3), 1.57-1.61 (m, 2H, CH_2), 1.70-1.74 (m, 4H, CH_2), 3.14-3.17 (m, 4H, CH_2), 4.20-4.25 (m, 4H, CH_2), 4.30-4.36 (m, 4H, CH_2), 7.22 (s, 1H, CH), 7.53 (s, 1H, CH), 7.59 ppm (s, 1H, CH). ^{13}C NMR (125 MHz, $CDCl_3$, 25 °C): δ = 14.17, 14.29, 14.32, 23.78, 25.67, 56.19, 61.46, 61.50, 61.86, 61.89, 118.65, 118.76, 121.95, 124.12, 133.93, 135.76, 136.52, 164.80, 164.91, 166.71, 166.97, 169.58 ppm. FT-IR (HATR): ν = 2922, 2851, 1616, 1540, 1417, 1348, 1137, 1110, 1051, 1002, 973, 885, 786 cm^{-1}. HR-MALDI-MS (DHB): calcd for $C_{25}H_{33}NO_8S$ $[M]^+$ 507.19214; found 507.19402.

Chromophore 3d. Aldehyde **9d** (276 mg) and diethyl malonate (400 mg) were dissolved in CH_2Cl_2 (15 ml), Al_2O_3 (510 mg; 5 mmol) and a few drops of piperidine were added. The reaction mixture was refluxed for 16 h, filtered, and the solvent was evaporated in *vacuo*. The crude product was purified by column chromatography (SiO_2, EtOAc/Hex 2:3 and CH_2Cl_2/EtOAc 20:1). Yield: 302 mg (54 %); red solid. R_f = 0.7 (SiO_2; EtOAc/Hex 2:3); mp 123 °C. Found: C, 61.97; H, 6.82; N, 2.47; S, 5.61; $C_{29}H_{37}NO_8S$ requires C, 62.23; H, 6.66; N, 2.50; S, 5.73 %. ^{1}H NMR (400 MHz, $CDCl_3$, 25 °C): δ = 1.29-1.38 (m, 12H, CH_3), 1.59-1.63 (m, 2H, CH_2), 1.72-1.78 (m, 4H, CH_2), 3.04-3.07 (m, 4H, CH_2), 4.22-4.28 (m, 4H, CH_2), 4.31-4.37 (m, 4H, CH_2), 6.86 (dd, J_1 = 11.6 Hz, J_2 = 14.8 Hz, 1H, CH), 6.93-7.02 (m, 3H, CH+CHth), 7.12 (s, 1H, CH), 7.44 (d, J = 11.6 Hz, 1H, CH), 7.48 ppm (dd, J_1 = 1.6 Hz, J_2 = 9.2 Hz, 1H, CH). ^{13}C NMR (125 MHz, $CDCl_3$, 25 °C): δ = 14.43, 14.50, 23.85, 25.82, 56.07, 61.41, 61.44, 61.46, 121.27, 121.85, 123.03, 123.33, 124.87, 129.26, 131.13, 136.40, 137.70, 145.86, 145.92, 146.67, 163.62, 165.23, 165.33, 165.71, 165.86 ppm. FT-IR (HATR): ν = 2978, 2936, 2854, 1718, 1587, 1443, 1375, 1208, 1144, 1058, 1021, 858 cm^{-1}. HR-MALDI-MS (DHB): calcd for $C_{29}H_{37}NO_8S$ $[M]^+$ 559.22344; found 559.22518.

Chromophore 4a. The title compound was synthesized from aldehyde **9a** (195 mg) and dimedone (168 mg) following the general method (iii). Yield: 260 mg (82 %); orange solid. R_f = 0.6 (SiO_2; CH_2Cl_2/EtOAc 1:1); mp 205 °C. Found: C, 68.02; H, 7.35; N, 4.40; S, 10.05; $C_{18}H_{23}NO_2S$ requires C, 68.10; H, 7.30; N, 4.41; S, 10.10 %. ^{1}H NMR (500 MHz, $CDCl_3$, 25 °C): δ = 1.05 (s, 6H, CH_3), 1.71 (s, 6H, CH_2), 2.44 (s, 4H, CH_2), 3.55-3.56 (m, 4H, CH_2), 6.33 (d, J = 5 Hz, 1H, CHth), 7.62 (d, J = 4.5 Hz, 1H, CHth), 8.12 ppm (s, 1H, CH). ^{13}C NMR (125 MHz, $CDCl_3$, 25 °C): δ = 23.82, 25.52, 28.82, 30.79, 51.28, 52.22, 108.94, 115.40, 123.77, 143.42, 152.75, 173.70, 197.24 ppm. FT-IR (HATR): ν = 2940, 2855, 1647, 1585, 1558, 1482, 1440, 1374, 1356, 1243, 1188, 1122, 1091, 1018, 890, 758 cm^{-1}. HR-MALDI-MS (DHB): calcd for $C_{18}H_{24}NO_2S$ $[M+H]^+$ 318.15223; found 318.15252.

Chromophore 4b. Aldehyde **9b** (221 mg) and dimedone (168 mg) were dissolved in CH_2Cl_2 (15 mL) and a few drops of piperidine were added. The reaction mixture was stirred at 25 °C for 16 h, the solvent was evaporated *in vacuo*, and the crude product was purified by column chromatography (SiO_2, CH_2Cl_2/EtOAc 1:1). Yield: 85 mg (25 %); violet solid. R_f = 0.8 (SiO_2; CH_2Cl_2/EtOAc 1:1); mp 169 °C. Found: C, 69.99; H, 7.51; N, 4.02; S, 9.11; $C_{20}H_{25}NO_2S$ requires C, 69.93; H, 7.34; N, 4.08; S, 9.34 %. ^{1}H NMR (500 MHz, $CDCl_3$, 25 °C): δ = 1.04 (s, 6H, CH_3), 1.64-1.73 (m, 6H, CH_2), 2.44 (s, 4H, CH_2), 3.38-3.40 (m, 4H, CH_2), 6.07 (d, J = 4.5 Hz, 1H, CHth), 7.19 (d, J = 4.5 Hz, 1H, CHth), 7.40 (d, J = 13.5 Hz, 1H, CH), 7.79 (d, J = 12.5 Hz, 1H, CH), 7.86-7.91 ppm (m, 1H, CH). ^{13}C NMR (125 MHz, $CDCl_3$, 25 °C): δ = 23.72, 25.22, 28.80, 30.59, 51.53, 106.30, 119.10, 122.33, 126.24, 139.92, 149.54, 152.94, 167.59, 198.37 ppm. FT-IR (HATR): ν = 2935, 2851, 1613, 1540, 1346, 1212, 1108, 1002, 784 cm^{-1}. HR-MALDI-MS (DHB): calcd for $C_{20}H_{26}NO_2S$ $[M+H]^+$ 344.16788; found 344.16822.

Chromophore 4c. Aldehyde **9c** (223 mg) and dimedone (350 mg) were dissolved in $CHCl_3$ (30 mL) and a few drops of piperidine were added. The reaction mixture was heated at 40 °C for 16 h, the solvent was evaporated *in vacuo*, the crude product was dissolved in EtOAc (5 mL), and precipitated with hexane. The precipitate was filtered off, subsequently purified by filtration through a short plug (SiO_2, EtOAc/Hex 2:1), and re-precipitated again from EtOAc/hexane. The product proved unstable on SiO_2. Yield: 61 mg (13 %); red-violet solid. R_f = 0.4 (SiO_2; EtOAc/Hex 2:1); mp 204 °C. Found: C, 67.21; H, 7.05; N, 2.98; S, 6.05; $C_{27}H_{33}NO_4S$ requires C, 67.35; H, 7.11; N, 3.00; S, 6.66 %. ^{1}H NMR (500 MHz, $CDCl_3$, 25 °C): δ = 1.07 (s, 6H, CH_3), 1.10 (s, 6H, CH_3), 1.74-1.81 (m, 6H, CH_2), 2.50 (s, 4H, CH_2), 2.56 (s, 2H, CH_2), 2.58 (s, 2H, CH_2), 3.62 (s, 4H, CH_2), 7.86 (s, 1H, CH), 8.14 (s, 1H, CH), 8.41 ppm (s, 1H, CH). ^{13}C NMR (125 MHz, $CDCl_3$, 25 °C): δ = 23.87, 26.03, 28.82, 28.84, 30.32, 30.55, 52.18, 52.58, 53.18, 54.25, 56.37, 119.01, 120.83, 123.00, 125.91, 141.88, 145.57, 152.68, 178.86, 197.48, 197.50, 198.43, 198.45 ppm. FT-IR (HATR): ν = 2930, 2860, 1648, 1624, 1467, 1351, 1288, 1233, 1201, 1133, 1116, 955, 646 cm^{-1}. HR-MALDI-MS (DHB): calcd for $C_{27}H_{34}NO_4S$ $[M+H]^+$ 468.22031; found 468.22239.

Chromophore 4d. The title compound was synthesized from dialdehyde **9d** (276 mg) and dimedone (350 mg) following the general method (ii). Yield: 210 mg (40 %); black solid. R_f = 0.85 (SiO_2; EtOAc/Hex 2:1). Found: C, 70.31; H, 7.29; N, 2.47; S, 5.59; $C_{31}H_{37}NO_4S$ requires C, 70.64; H, 7.18; N, 2.70; S, 6.17 %. ^{1}H NMR (500 MHz, $CDCl_3$, 25 °C): δ = 1.05-1.06 (2×s, 12H, CH_3), 1.67-1.69 (m, 2H, CH_2), 1.76-1.81 (m, 4H, CH_2), 2.49-2.51 (m, 8H, CH_2), 3.29-3.31 (m, 4H, CH_2), 7.22 (d, J = 15 Hz, 1H, CH), 7.33 (d, J = 15 Hz, 1H, CH), 7.39 (s, 1H, CHth), 7.74 (t, J = 12.5 Hz, 2H, CH), 7.93 (dd, J_1 = 12 Hz, J_2 = 14.5 Hz, 1H, CH), 8.03 ppm (dd, J_1 = 12.5 Hz, J_2 = 15 Hz, 1H, CH). ^{13}C NMR (125 MHz, $CDCl_3$, 25 °C): δ = 23.76, 25.65, 28.76, 30.40, 52.42, 52.47, 54.13, 55.97, 123.31, 123.41, 123.80, 126.62, 126.92, 129.75, 133.76, 145.39, 146.33, 151.39, 152.45, 168.62, 198.06, 198.36, 199.16, 199.22 ppm. FT-IR (HATR): ν = 2934, 2865, 2359, 1642, 1549, 1486, 1367, 1234, 1134, 973, 777 cm^{-1}. HR-MALDI-MS (DHB): calcd for $C_{31}H_{38}NO_4S$ $[M+H]^+$ 520.25161; found 520.25237.

Chromophore 5a. The title compound was synthesized from aldehyde **9a** (195 mg) and Meldrum´s acid (172 mg) following the general method (iii) in CH_2Cl_2 at 25 °C. Yield: 128 mg (40 %); orange solid. R_f = 0.4 (SiO_2; Hex/EtOAc 1:2); mp 184 °C. Found: C, 59.87; H, 6.02; N, 4.36; S, 9.89; $C_{16}H_{19}NO_4S$ requires C, 59.79; H, 5.96; N, 4.36; S, 9.98 %. ^{1}H NMR (400 MHz, $CDCl_3$, 25 °C): δ = 1.71-1.73 (m, 12H, CH_2+CH_3), 3.55-3.56 (m, 4H,

CH_2), 6.28 (d, J = 5.2 Hz, 1H, CHth), 7.56 (d, J = 4.8 Hz, 1H, CHth), 8.22 ppm (s, 1H, CH). ^{13}C NMR (125 MHz, $CDCl_3$, 25 °C): δ = 23.77, 25.54, 27.45, 51.56, 92.97, 103.58, 107.98, 122.10, 146.56, 151.91, 163.65, 165.76, 175.00 ppm. FT-IR (HATR): ν = 2923, 2854, 1672, 1493, 1372, 1256, 1177, 1005, 929, 770 cm^{-1}. HR-MALDI-MS (DHB): calcd for $C_{16}H_{20}NO_4S$ $[M+H]^+$ 322.11075; found 322.13881.

Chromophore 5b. The title compound was synthesized from aldehyde **9b** (221 mg) and Meldrum´s acid (216 mg; 1.5 mmol) following the general method (ii) in CH_3CN at 85 °C for 48 h. Yield: 153 mg (44 %); violet solid. R_f = 0.6 (SiO_2; Hex/EtOAc 1:2); mp 213 °C. Found: C, 62.13; H, 6.15; N, 4.01; S, 9.07; $C_{18}H_{21}NO_4S$ requires C, 62.23; H, 6.09; N, 4.03; S, 9.23 %. ^{1}H NMR (400 MHz, $CDCl_3$, 25 °C): δ= 1.70-1.73 (m, 12H, CH_2+CH_3), 3.42-3.45 (m, 4H, CH_2), 6.12 (d, J = 4.8 Hz, 1H, CHth), 7.27 (d, J = 4.8 Hz, 1H, CHth), 7.38 (d, J = 14 Hz, 1H, CH), 7.58 (t, J = 13.2 Hz, 1H, CH), 8.00 ppm (d, J = 12.8 Hz, 1H, CH). ^{13}C NMR (100 MHz, $CDCl_3$, 25 °C): δ = 23.72, 25.30, 27.53, 51.72, 100.88, 103.79, 106.92, 117.59, 125.48, 141.61, 149.09, 157.61, 162.69, 164.97, 168.87 ppm. FT-IR (HATR): ν = 2852, 2358, 1673, 1514, 1469, 1410, 1349, 1210, 1138, 1112, 987, 927, 758 cm^{-1}. HR-MALDI-MS (DHB): calcd for $C_{18}H_{21}NO_4S$ $[M]^+$ 347.11858; found 347.11969.

Chromophore 5c. The title compound was synthesized from aldehyde **9c** (222 mg) and Meldrum´s acid (360 mg) following the general method (iii) in CH_2Cl_2 at 25 °C. Yield: 180 mg (38 %); red-violet solid. R_f = 0.75 (SiO_2; EtOAc/CH_2Cl_2 1:10); mp 199 °C. Found: C, 57.02; H, 5.04; N, 2.72; S, 5.91; $C_{23}H_{25}NO_8S$ requires C, 58.09; H, 5.30; N, 2.95; S, 5,74 %. ^{1}H NMR (400 MHz, $CDCl_3$, 25 °C): δ = 1.73 (s, 6H, CH_3), 1.75 (s, 8H, CH_2+CH_3), 1.84-1.86 (m, 4H, CH_2), 3.67-3.69 (m, 4H, CH_2), 8.23 (s, 1H, CH), 8.35 (s, 1H, CH), 8.41 ppm (s, 1H, CH). ^{13}C NMR (125 MHz, $CDCl_3$, 25 °C): δ = 23.66, 25.99, 27.60, 27.85, 56.85, 102.19, 104.59, 104.62, 107.03, 116.75, 122.44, 147.41, 149.57, 151.53, 160.90, 162.44, 163.99, 179.62 ppm. FT-IR (HATR): ν = 2921, 2852, 2364, 1690, 1490, 1356, 1271, 1154, 1020, 920, 787 cm^{-1}. HR-MALDI-MS (DHB): calcd for $C_{23}H_{25}NO_8S$ $[M]^+$ 475.12954; found 475.13067.

Chromophore 5d. The title compound was synthesized from dialdehyde **9d** (276 mg) and Meldrum´s acid (360 mg) following the general method (ii). Yield: 460 mg (87 %); black solid. R_f = 0.8 (SiO_2; EtOAc/CH_2Cl_2 1:20). Found: C, 61.21; H, 5.64; N, 2.64; S, 5.91; $C_{27}H_{29}NO_8S$ requires C, 61.47; H, 5.54; N, 2.65; S, 6.08 %. ^{1}H NMR (400 MHz, $CDCl_3$, 25 °C): δ = 1.73-1.74 (m, 14H, CH_2+CH_3), 1.80-1.85 (m, 4H, CH_2), 3.39-3.42 (m, 4H, CH_2), 7.27 (d, J = 15.6 Hz, 1H, CH), 7.38 (d, J = 14.8 Hz, 1H, CH), 7.49 (s, 1H, CHth), 7.77 (dd, J_1 = 12 Hz, J_2 = 14.8 Hz, 1H, CH), 7.93 (dd, J_1 = 12 Hz, J_2 = 14.8 Hz, 1H, CH), 8.08 ppm (dd, J_1 = 12 Hz, J_2 = 16 Hz, 2H, CH). ^{13}C NMR (125 MHz, $CDCl_3$, 25 °C): δ= 23.68, 25.63, 27.79, 56.11, 104.65, 104.75, 108.20, 108.39, 122.24, 122.68, 128.69, 135.42, 145.75, 146.45, 157.37, 158.49, 161.45, 161.54, 163.60, 163.76, 170.30 ppm. FT-IR (HATR): ν = 2931, 2358, 1703, 1556, 1453, 1354, 1277, 1141, 1106, 991, 926, 787, 715 cm^{-1}. HR-MALDI-MS (DHB): calcd for $C_{27}H_{29}NO_8S$ $[M]^+$ 527.16084; found 527.16244.

Chromophore 6a. The title compound was synthesized from aldehyde **9a** (195 mg) and *N*,*N´*-dibutylbarbituric acid (288 mg) following the general method (iii) in CH_2Cl_2 at 25 °C. Yield: 260 mg (62 %); orange solid. R_f = 0.8 (SiO_2; CH_2Cl_2/acetone 100:5); mp 172 °C. Found: C, 63.32; H, 7.52; N, 10.04; S, 7.61; $C_{22}H_{31}N_3O_3S$ requires C, 63.28; H, 7.48; N, 10.06; S, 7.68 %. ^{1}H NMR (500 MHz, $CDCl_3$, 25 °C): δ = 0.93 (t, J = 7.5 Hz, 6H, CH_3), 1.34-1.38 (m, 4H, CH_2), 1.60-1.72 (m, 10H, CH_2), 3.56-3.57 (m, 4H, CH_2), 3.91-3.94 (m, 4H, CH_2), 6.31 (d, J = 5 Hz, 1H, CHth), 7.60 (s, 1H, CHth), 8.30 ppm (s, 1H, CH). ^{13}C NMR (125 MHz, $CDCl_3$, 25 °C): δ= 14.09, 20.46, 23.75, 25.55, 30.54, 41.03, 41.77, 51.37, 99.65, 108.25, 122.67, 146.42, 151.92, 151.96, 162.85, 163.90, 174.74 ppm. FT-IR (HATR): ν = 2923, 2856, 1632, 1470, 1411, 1248, 1155, 1084, 783 cm^{-1}. HR-MALDI-MS (DHB): calcd for $C_{22}H_{32}N_3O_3S$ $[M+H]^+$ 418.21589; found 418.21567.

Chromophore 6b. Aldehyde **9b** (222 mg) and *N*,*N´*-dibutylbarbituric acid (288 mg) were dissolved in 1,2-dichloroethane (20 mL) and Al_2O_3 (255 mg; 2.5 mmol) was added. The reaction mixture was refluxed for 6 h, subsequently stirred at 25 °C for 16 h, filtered, and the solvent was evaporated *in vacuo*. The crude product was purified by column chromatography (SiO_2, CH_2Cl_2/acetone 60:1). Yield: 248 mg (56 %); black solid. R_f = 0.4 (SiO_2; CH_2Cl_2); mp 148 °C. Found: C, 64.70; H, 7.56; N, 9.21; S, 6.98; $C_{24}H_{33}N_3O_3S$ requires C, 64.98; H, 7.50; N, 9.47; S, 7.23 %. ^{1}H NMR (400 MHz, $CDCl_3$, 25 °C): δ = 0.90-0.93 (m, 6H, CH_3), 1.31-1.38 (m, 4H, CH_2), 1.56-1.61 (m, 4H, CH_2), 1.63-1.70 (m, 6H, CH_2), 3.38-3.40 (m, 4H, CH_2), 3.88-3.92 (m, 4H, CH_2), 6.08 (d, J = 4.8 Hz, 1H, CHth), 7.22 (d, J = 4.4 Hz, 1H, CHth), 7.38 (d, J = 13.6 Hz, 1H, CH), 7.88 (t, J = 13.2 Hz, 1H, CH), 8.01 ppm (d, J = 12.8 Hz, 1H, CH). ^{13}C NMR (125 MHz, $CDCl_3$, 25 °C): δ = 13.87, 13.90, 20.24, 20.35, 23.53, 25.07, 30.32, 30.40, 40.99, 41.50, 51.47, 106.25, 106.60, 118.06, 125.73, 140.89, 148.86, 151.59, 156.63, 162.49, 163.14, 168.19 ppm. FT-IR (HATR): ν = 2936, 2850, 1703, 1632, 1553, 1513, 1401, 1359, 1331, 1214, 1133, 1051, 993, 884, 748 cm^{-1}. HR-MALDI-MS (DHB): calcd for $C_{24}H_{34}N_3O_3S$ $[M+H]^+$ 444.23154; found 444.23174.

Chromophore 6c. The title compound was synthesized from aldehyde **9c** (222 mg) and *N*,*N´*-dibutylbarbituric acid (600 mg) following the general method (iii) at 25 °C for 3 h. Yield: 448 mg (67 %); dark red solid. R_f = 0.3 (SiO_2; CH_2Cl_2); mp 127 °C. Found: C, 63.19; H, 7.62; N, 10.20; S, 4.61; $C_{35}H_{49}N_5O_6S$ requires C, 62.94; H, 7.40; N, 10.49; S, 4.80 %. ^{1}H NMR (400 MHz, $CDCl_3$, 25 °C): δ= 0.93-0.99 (m, 12H, CH_3), 1.34-1.43 (m, 8H, CH_2), 1.58-1.62 (m, 8H, CH_2), 1.76-1.86 (m, 6H, CH_2), 3.66-3.68 (m, 4H, CH_2), 3.91-3.97 (m, 8H, CH_2), 8.26 (s, 1H, CH), 8.46 (s, 1H, CH), 8.62 ppm (s, 1H, CH). ^{13}C NMR (125 MHz, $CDCl_3$, 25 °C): δ= 13.93, 13.98, 20.29, 20.32, 20.35, 20.37, 23.70, 26.09, 30.27, 30.31, 41.31, 41.78, 42.03, 42.35 56.68, 106.50, 111.33, 118.06, 122.51, 147.09, 149.40, 151.00, 151.25, 152.37, 160.90, 162.28, 162.79, 162.89, 180.13 ppm. FT-IR (HATR): ν = 2954, 2870, 1654, 1535, 1389, 1365, 1287, 1149, 1100, 950, 787 cm^{-1}. HR-MALDI-MS (DHB): calcd for $C_{35}H_{50}N_5O_6S$ $[M+H]^+$ 668.34763; found 668.34758.

Chromophore 6d. The title compound was synthesized from dialdehyde **9d** (276 mg) and *N*,*N´*-dibutylbarbituric acid (600 mg) following the general method (ii). Yield: 634 mg (88 %); black solid. R_f = 0.55 (SiO_2; CH_2Cl_2). Found: C, 65.15; H, 7.54; N, 9.69; S, 4.38; $C_{39}H_{53}N_5O_6S$ requires C, 65.06; H, 7.42; N, 9.73; S, 4.45 %. ^{1}H NMR (400 MHz, $CDCl_3$, 25 °C): δ = 0.94-0.97 (m, 12H, CH_3), 1.32-1.43 (m, 8H, CH_2), 1.58-1.64 (m, 8H, CH_2), 1.71-1.81 (m, 6H, CH_2), 3.37-3.40 (m, 4H, CH_2), 3.90-3.95 (m, 8H, CH_2), 7.27 (d, J = 13.6 Hz, 1H, CH), 7.32-7.39 (m, 1H, CH), 7.52 (s, 1H, CHth), 8.06-8.12 (m, 3H, CH), 8.22 ppm (dd, J_1 = 12.4 Hz, J_2 = 14.8 Hz, 1H, CH). ^{13}C NMR (125 MHz, $CDCl_3$, 25 °C): δ= 13.99, 14.03, 20.37, 20.47, 23.75, 25.68, 30.39, 30.46, 41.53, 41.56, 42.06, 56.12, 112.23, 112.51, 122.80, 122.91, 123.24, 129.26, 134.57, 145.35, 146.26, 151.26, 151.30, 156.57, 157.56, 162.00, 162.09, 162.55, 162.70, 169.66 ppm. FT-IR (HATR): ν = 2954, 2864, 2360, 1654, 1558, 1496, 1402, 1370, 1152, 1102, 987, 789 cm^{-1}. HR-MALDI-MS (DHB): calcd for $C_{39}H_{54}N_5O_6S$ $[M+H]^+$ 720.37893; found 720.37825.

Chromophore 7a. The title compound was synthesized from aldehyde **9a** (196 mg) and *N*,*N´*-dibutyl-2-thiobarbituric acid (308 mg) following the general method (iii) at 25 °C. Yield: 252 mg (58 %); pink-red solid. R_f = 0.65 (SiO_2; CH_2Cl_2); mp 216 °C. Found: C, 61.21; H, 7.33; N, 9.54; S, 14.51; $C_{22}H_{31}N_3O_2S_2$ requires C, 60.94; H, 7.21; N, 9.69; S, 14.79 %. ^{1}H NMR (500 MHz, $CDCl_3$, 25 °C): δ= 0.93-0.96 (m, 6H, CH_3), 1.36-1.42 (m, 4H, CH_2), 1.69-1.75 (m, 10H, CH_2), 3.61-3.62 (m, 4H, CH_2), 4.45-4.50 (m, 4H, CH_2), 6.39 (d, J = 5 Hz, 1H, CHth), 7.63 (d, J = 5 Hz, 1H, CHth),

8.28 ppm (s, 1H, CH). ^{13}C NMR (125 MHz, $CDCl_3$, 25 °C): δ = 14.10, 14.15, 20.47, 23.73, 25.66, 29.35, 47.49, 48.36, 51.70, 100.47, 109.59, 123.97, 146.53, 152.83, 161.08, 162.49, 175.84, 178.92 ppm. FT-IR (HATR): ν = 2919, 2851, 1630, 1484, 1412, 1381, 1239, 1151, 1105, 995, 947, 886, 778 cm^{-1}. HR-MALDI-MS (DHB): calcd for $C_{22}H_{32}N_3O_2S_2$ $[M+H]^+$ 434.19304; found 434.19302.

Chromophore 7b. The title compound was synthesized from aldehyde **9b** (221 mg) and *N,N´*-dibutyl-2-thiobarbituric acid (307 mg) following the general method (ii) at 40 °C. Yield: 261 mg (57 %); dark green solid. R_f = 0.4 (SiO_2; CH_2Cl_2); mp 175 °C. Found: C, 62.69; H, 7.31; N, 8.98; S, 13.81; $C_{24}H_{33}N_3O_2S_2$ requires C, 62.71; H, 7.24; N, 9.14; S, 13.95 %. ^{1}H NMR (400 MHz, $CDCl_3$, 25 °C): δ = 0.93-0.97 (m, 6H, CH_3), 1.35-1.43 (m, 4H, CH_2), 1.68-1.73 (m, 10H, CH_2), 3.47-3.48 (m, 4H, CH_2), 4.44-4.48 (m, 4H, CH_2), 6.19 (d, J = 4.8 Hz, 1H, CHth), 7.33 (d, J = 4 Hz, 1H, CHth), 7.46 (d, J = 13.6 Hz, 1H, CH), 7.93 (t, J = 13.2 Hz, 1H, CH), 8.04 ppm (d, J = 12.8 Hz, 1H, CH). ^{13}C NMR (125 MHz, $CDCl_3$, 25 °C): δ = 14.09, 14.11, 20.45, 20.51, 23.69, 25.37, 29.37, 29.42, 47.71, 48.20, 52.00, 106.27, 108.10, 118.89, 126.43, 150.07, 157.26, 161.05, 162.07, 169.99, 178.96 ppm. FT-IR (HATR): ν = 2921, 2851, 1633, 1508, 1336, 1206, 1104, 1051, 986 cm^{-1}. HR-MALDI-MS (DHB): calcd for $C_{24}H_{33}N_3O_2S_2$ $[M]^+$ 459.20087; found 459.20101.

Chromophore 7c. The title compound was synthesized from aldehyde **9c** (222 mg) and *N,N´*-dibutyl-2-thiobarbituric acid (640 mg) following the general method (iii) at 25 °C. Yield: 440 mg (63 %); dark brown solid. R_f = 0.6 (SiO_2; CH_2Cl_2/Hex 4:1); mp 172 °C. Found: C, 60.01; H, 7.13; N, 9.95; S, 13.57; $C_{35}H_{49}N_5O_4S_3$ requires C, 60.05; H, 7.06; N, 10.00; S, 13.74 %. ^{1}H NMR (400 MHz, $CDCl_3$, 25 °C): δ = 0.93-0.99 (m, 12H, CH_3), 1.35-1.42 (m, 8H, CH_2), 1.66-1.70 (m, 8H, CH_2), 1.78-1.88 (m, 6H, CH_2), 3.70-3.73 (m, 4H, CH_2), 4.41-4.46 (m, 8H, CH_2), 8.25 (s, 1H, CH), 8.44 (s, 1H, CH), 8.66 ppm (s, 1H, CH). ^{13}C NMR (125 MHz, $CDCl_3$, 25 °C): δ = 14.02, 14.08, 20.37, 20.39, 20.40, 23.70, 26.21, 29.23, 47.70, 48.34, 48.55, 48.80, 56.83, 107.26, 112.00, 118.95, 123.30, 148.18, 150.37, 153.16, 159.18, 160.59, 161.49, 161.58, 179.11, 179.13, 180.67 ppm. FT-IR (HATR): ν = 2927, 2855, 1655, 1529, 1477, 1365, 1281, 1198, 1153, 1118, 948, 783 cm^{-1}. HR-MALDI-MS (DHB): calcd for $C_{35}H_{50}N_5O_4S_3$ $[M+H]^+$ 700.30194; found 700.30096.

Chromophore 7d. The title compound was synthesized from dialdehyde **9d** (276 mg) and *N,N´*-dibutyl-2-thiobarbituric acid (640 mg) following the general method (ii) in CH_3CN. Yield: 609 mg (81 %); black solid. R_f = 0.8 (SiO_2; CH_2Cl_2). Found: C, 62.34; H, 7.21; N, 9.20; S, 12.49; $C_{39}H_{53}N_5O_4S_3$ requires C, 62.28; H, 7.10; N, 9.31; S, 12.79 %. ^{1}H NMR (400 MHz, $CDCl_3$, 25 °C): δ = 0.93-0.98 (m, 12H, CH_3), 1.35-1.43 (m, 8H, CH_2), 1.64-1.82 (m, 14H, CH_2), 3.45-3.48 (m, 4H, CH_2), 4.41-4.45 (m, 8H, CH_2), 7.30 (d, J = 14.8 Hz, 1H, CH), 7.35-7.41 (m, 1H, CH), 7.43 (s, 1H, CHth), 8.01-8.11 (m, 3H, CH), 8.22 ppm (dd, J_1 = 12.4 Hz, J_2 = 14.4 Hz, 1H, CH). ^{13}C NMR (125 MHz, $CDCl_3$, 25 °C): δ = 14.01, 14.03, 20.36, 20.43, 23.67, 25.68, 29.26, 29.28, 29.32, 47.90, 47.95, 48.39, 56.16, 112.51, 112.80, 122.62, 123.45, 123.73, 128.98, 135.63, 146.24, 147.05, 157.65, 158.63, 160.25, 160.34, 161.15, 161.29, 170.64, 179.22, 179.25 ppm. FT-IR (HATR): ν = 2956, 2860, 1663, 1551, 1468, 1371, 1294, 1198, 1154, 1123, 1089, 984, 956, 785 cm^{-1}. HR-MALDI-MS (DHB): calcd for $C_{39}H_{54}N_5O_4S_3$ $[M+H]^+$ 752.33324; found 752.33270.

Chromophore 8a. The title compound was synthesized from aldehyde **9a** (195 mg) and indan-1,3-dione (175 mg) following the general method (iii) at 25 °C. Yield: 226 mg (70 %); dark green-red solid. R_f = 0.6 (SiO_2; CH_2Cl_2/EtOAc 10:1); mp 182 °C. Found: C, 70.44; H, 5.52; N, 4.32; S, 9.79; $C_{19}H_{17}NO_2S$ requires C, 70.56; H, 5.30; N, 4.33; S, 9.91 %. ^{1}H NMR (500 MHz, $CDCl_3$, 25 °C): δ = 1.70-1.72 (m, 6H, CH_2), 3.52-3.54 (m, 4H, CH_2), 6.23 (d, J = 5 Hz, 1H, CHth), 7.59-7.61 (m, 3H, CHth+CHind), 7.71 (s, 1H, CH), 7.75-7.77 ppm (m, 2H, CHind). ^{13}C NMR (125 MHz, $CDCl_3$, 25 °C): δ = 23.69, 25.36, 51.38, 107.59, 114.70, 121.45, 121.75, 133.40, 133.60, 136.55, 140.34, 141.44, 149.46, 172.78, 190.82, 191.74 ppm. FT-IR (HATR): ν = 2922, 2850, 1643, 1561, 1483, 1406, 1376, 1249, 1195, 1103, 1078, 746 cm^{-1}. HR-MALDI-MS (DHB): calcd for $C_{19}H_{18}NO_2S$ $[M+H]^+$ 324.10528; found 324.10454.

Chromophore 8b. The title compound was synthesized from aldehyde **9b** (221 mg) and indan-1,3-dione (175 mg) following the general method (ii) at 40 °C for 48 h. Yield: 178 mg (51 %); tawny solid. R_f = 0.7 (SiO_2; CH_2Cl_2/EtOAc 20:1); mp 204 °C. Found: C, 72.04; H, 5.57; N, 3.97; S, 8.95; $C_{21}H_{19}NO_2S$ requires C, 72.18; H, 5.48; N, 4.01; S, 9.18 %. ^{1}H NMR (500 MHz, $CDCl_3$, 25 °C): δ = 1.66-1.71 (m, 6H, CH_2), 3.37-3.39 (m, 4H, CH_2), 6.06 (t, J = 4.5 Hz, 1H, CHth), 7.17 (d, J = 1.5 Hz, 1H, CHth), 7.33 (dd, J_1 = 2 Hz, J_2 = 14.5 Hz, 1H, CH), 7.51 (dd, J_1 = 2.5 Hz, J_2 = 12.5 Hz, 1H, CH), 7.62-7.65 (m, 2H, CHind), 7.74 (dd, J_1 = 3 Hz, J_2 = 14.5 Hz, 1H, CH), 7.80-7.82 ppm (m, 2H, CHind). ^{13}C NMR (125 MHz, $CDCl_3$, 25 °C): δ = 23.74, 25.20, 51.51, 106.04, 117.32, 121.67, 122.01, 122.30, 126.15, 133.92, 134.11, 138.98, 140.77, 142.09, 146.04, 146.33, 166.92, 191.37, 191.67 ppm. FT-IR (HATR): ν = 2921, 2852, 1642, 1561, 1517, 1418, 1350, 1210, 1101, 1058, 986, 738 cm^{-1}. HR-MALDI-MS (DHB): calcd for $C_{21}H_{20}NO_2S$ $[M+H]^+$ 350.12093; found 350.12039.

Chromophore 8c. The title compound was synthesized from aldehyde **9c** (222 mg) and indan-1,3-dione (366 mg) following the general method (iii) at 25 °C. Yield: 398 mg (83 %); dark brown solid. R_f = 0.6 (SiO_2; CH_2Cl_2/EtOAc 10:1); mp 243 °C. Found: C, 72.56; H, 4.49; N, 2.91; S, 6.64; $C_{29}H_{21}NO_4S$ requires C, 72.63; H, 4.41; N, 2.92; S, 6.69 %. ^{1}H NMR (500 MHz, $CDCl_3$, 25 °C): δ = 1.78-1.80 (m, 2H, CH_2), 1.87-1.89 (m, 4H, CH_2), 3.69-3.72 (m, 4H, CH_2), 7.68 (s, 1H, CH), 7.71-7.72 (m, 2H, CHind), 7.76-7.78 (m, 2H, CHind), 7.86-7.88 (m, 1H, CHind), 7.89-7.93 (m, 3H, CH+CHind), 7.96-7.98 (m, 1H, CHind), 9.00 ppm (s, 1H, CH). ^{13}C NMR (125 MHz, $CDCl_3$, 25 °C): δ = 23.83, 25.92, 56.80, 118.75, 121.20, 122.56, 122.88, 123.00, 123.17, 123.45, 123.57, 134.74, 134.97, 134.99, 135.26, 137.74, 140.20, 140.73, 141.80, 142.48, 149.95, 178.48, 189.74, 190.65, 190.66, 191.06 ppm. FT-IR (HATR): ν = 3070, 2929, 2850, 1676, 1552, 1486, 1383, 1328, 1279, 1179, 1151, 1102, 944, 878, 727, 676 cm^{-1}. HR-MALDI-MS (DHB): calcd for $C_{29}H_{22}NO_4S$ $[M+H]^+$ 480.12641; found 480.12666.

Chromophore 8d. The title compound was synthesized from dialdehyde **9d** (256 mg) and indan-1,3-dione (366 mg) following the general method (ii) in CH_3CN. Chromophore **8d** is sparingly soluble in chlorinated solvents. Yield: 430 mg (81 %); black gold solid. R_f = 0.75 (SiO_2; CH_2Cl_2/CH_3OH 50:1). Found: C, 72.97; H, 5.00; N, 2.41; S, 5.64; $C_{33}H_{25}NO_4S$ requires C, 73.56; H, 4.74; N, 2.63; S, 6.03 %. ^{1}H NMR (400 MHz, CD_2Cl_2, 25 °C): δ = 1.71-1.74 (m, 2H, CH_2), 1.81-1.87 (m, 4H, CH_2), 3.36-3.39 (m, 4H, CH_2), 7.24 (d, J = 15.2 Hz, 1H, CH), 7.37 (d, J = 14.8 Hz, 1H, CH), 7.50-7.57 (m, 3H, CH+CHth), 7.72-7.80 (m, 4H, CHind), 7.86-7.94 (m, 5H, CH+CHind), 8.05 ppm (dd, J_1 = 12 Hz, J_2 = 15.2 Hz, 1H, CH). ^{13}C NMR (125 MHz, CD_2Cl_2, 25 °C): δ = 24.13, 26.08, 56.35, 121.43, 122.02, 122.89, 122.99, 123.07, 123.44, 126.23, 126.40, 129.85, 133.64, 133.66, 135.13, 135.19, 135.25, 135.36, 141.27, 141.30, 142.59, 142.60, 143.21, 144.04, 144.45, 145.61, 168.73, 190.49, 190.66, 191.08, 191.10 ppm. FT-IR (HATR): ν = 3499, 2917, 2850, 1673, 1563, 1478, 1320, 1235, 1154, 1143, 983, 733 cm^{-1}. HR-MALDI-MS (DHB): calcd for $C_{33}H_{26}NO_4S$ $[M+H]^+$ 532.15771; found 532.15699.

Acknowledgements

This research was supported by the Technology Agency of the Czech Republic (TE01020022, Flexprint). M. L. and F. B. are

indebted to the Ministry of Education, Youth and Sports of the Czech Republic (LG 15030).

Keywords: malonic acid • chromophore • charge-transfer • withdrawing strength • structure-property relationships

[1] W. B. Jensen, *J. Chem. Educ.* **2007**, *84*, 924.

[2] H. Strittmatter, S. Hildbrand, P. Pollak, Malonic Acid and Derivatives. *Ullmann's Encyclopedia of Industrial Chemistry.* **2012**, *22*, 157-174.

[3] a) P. Pollak, G. Romeder, Malonic Acid and Derivatives. *Kirk-Othmer Encyclopedia of Chemical Technology.* **2000**, 1-22.

[4] a) R. Menegatti, Green Chemistry – Aspects for the Knoevenagel Reaction in M. Kidwai, N. K. Mishra *(Eds.), Green Chemistry - Environmentally Benign Approaches.* **2012**, 13-32, InTech, Croatia; b) G. Jones, The Knoevenagel Condensation in S. E. Denmark (Ed.), *Organic Reactions*. **2011**, 204-599, John Wiley & Sons, Germany; c) A. M. Asiri, S. A. Khan, H. M. Basisi, *Int. J. Electrochem. Sci.* **2015**, *10*, 6092-6105.

[5] a) S. R. Forrest, M. E. Thompson, *Chem. Rev.* **2007**, *107*, 923-1386; b) R. D. Miller, E. A. Chandross, *Chem. Rev.* **2010**, *110*, 1-574; c) G. S. He, L.-S. Tan, Q. Zheng, P. N. Prasad, *Chem. Rev*. **2008**, *108*, 1245-1330; d) Y. Ohmori, *Laser Photonics Rev*. **2010**, *4*, 300-310.

[6] a) J. Kulhánek, F. Bureš, J. Opršal, W. Kuznik, T. Mikysek, A. Růžička, *Asian J. Org. Chem.* **2013**, *2*, 422-431; b) P. D. Jarowski, Y. Mo, *Chem. Eur. J.* **2014**, *20*, 17214-17221; c) H. Meier, *Angew. Chem. Int. Ed.* **2005**, *44*, 2482-2506; d) J. Y. Lee, K. S. Kim, B. J. Mhin, *J. Chem. Phys.* **2001**, *115*, 9484-9489; e) F. Bureš, O. Pytela, M. Kivala, F. Diederich, *J. Phys. Org. Chem.* **2011**, *24*, 274-281.

[7] F. Bureš, *RSC Adv.* **2014**, *4*, 58826-58851.

[8] a) H. S. Nalwa, *Adv. Mater.* **1993**, *5*, 341-358; b) T. Verbiest, S. Houbrechts, M. Kauranen, K. Clays, A. Persoons, *J. Mater. Chem.* **1997**, *7*, 2175-2189; c) D. F. Eaton, *Science.* **1991**, *253*, 281-287; d) L. R. Dalton, P. A. Sullivan, D. H. Bale, *Chem. Rev.* **2010**, *110*, 25-55.

[9] a) P. Batail, *Chem. Rev.* **2004**, *104*, 4887-4890; b) S. Allard, M. Forster, B. Souharce, H. Thiem, U. Scherf, *Angew. Chem., Int. Ed.* **2008**, *47*, 4070-4098.

[10] a) K. Hara, T. Sato, R. Katoh, A. Furube, Y. Ohga, A. Shinpo, *J. Phys. Chem. B.* **2003**, *107*, 597-606; b) K. Hara, T. Sato, R. Katoh, A. Furube, T. Yoshihara, M. Murai, M. Kurashige, S. Ito, A. Shinpo, S. Suga, H. Arakawa, *Adv. Funct. Mater.* **2005**, *15*, 246-252; c) L. Giribabu, M. Chandrasekheram, M. L. Kantham, V. G. Reddy, D. Satyanarayana, O. S. Rao, P. Y. Reddy, *Indian J. Chem., Sect A.* **2006**, *45*, 629-634; d) G. Li, K.-J. Jiang, Y.-F. Li, S.-L. Li, L.-M. Yang, *J. Phys. Chem. C.* **2008**, *112*, 11591-11599; e) K. Srinivas, K. Yesudas, K. Bhanuprakash, V. J. Rao, L. Giribabu, *J. Phys. Chem. C.* **2009**, *113*, 20117-20126; f) K. S. V. Gupta, J. Zhang, G. Marotta, M. A. Reddy, S. P. Singh, A. Islam, L. Han, F. De Angelis, M. Chandrasekharam, M. Pastore, *Dyes Pigments.* **2015**, *113*, 536-545; g) G. S. Reddy, S. Ramkumar, A. M. Asiri, S. Anandan, *Spectrochim. Acta A.* **2015**, *145*, 531-539; h) Y. Wu, W. Zhu, *Chem. Soc. Rev.* **2013**, *42*, 2039-2058.

[11] F. Freeman, *Chem. Rev.* **1969**, *69*, 591-624.

[12] a) M. Kivala, F. Diederich, *Acc. Chem. Res.* **2009**, *42*, 235-248; b) F. Bureš, W. B. Schweizer, J. C. May, C. Boudon, J.-P. Gisselbrecht, M. Gross, I. Biaggio, F. Diederich, *Chem. Eur. J.* **2007**, *13*, 5378-5387; c) J. C. May, I. Biaggio, F. Bureš, F. Diederich, *Appl. Phys. Lett.* **2007**, *90*, 251106; d) F. Bureš, O. Pytela, F. Diederich, *J. Phys.Org. Chem.* **2009**, *22*, 155-162; e) F. Bureš, W. B. Schweizer, C. Boudon, J.-P. Gisselbrecht, M. Gross, F. Diederich, *Eur. J. Org. Chem.* **2008**, *6*, 994-1004; f) Y.-L. Wu, F. Bureš, P. D. Jarowski, W. B. Schweizer, C. Boudon, J.-P. Gisselbrecht, F. Diederich, *Chem. Eur. J.* **2010**, *16*, 9592-9605; g) F. Bureš, O. Pytela, M. Kivala, F. Diederich, *J. Phys. Org. Chem.* **2011**, *24*, 274-281; h) A. Wojciechowski, M. M. M. Raposo, M. C. R. Castro, W. Kuznik, I. Fuks-Janczarek, M. Pokladko-Kowar, F. Bureš, *J. Mater. Sci.: Mater. Electron.* **2014**, *25*, 1745-1750.

[13] F. Bureš, *Chem. Listy* **2013**, *107*, 834-842.

[14] D. Cvejn, E. Michail, I. Polyzos, N. Almonasy, O. Pytela, M. Klikar, T. Mikysek, V. Giannetas, M. Fakis, F. Bureš, *J. Mater. Chem. C.* **2015**, *3*, 7345-7355.

[15] a) W. Zou, Y. Liu, Q. Jia, Z. Ge, *Chinese J. Org. Chem.* **2013**, *33*, 1522-1526; b) R. V. Pereira, M. H. Gehlen, *Chem. Phys. Lett.* **2006**, *426*, 311-317; c) C. Coluccini, A. K. Sharma, M. Caricato, A. Sironi, E. Cariati, S. Righetto, E. Tordin, C. Botta, A. Forni, D. Pasini, *Phys. Chem. Chem. Phys.* **2013**, *15*, 1666-1674; d) H. Mokbel, F. Dumur, S. Telitel, L. Vidal, P. Xiao, D.-L. Versace, M.-A. Tehfe, F. Morlet-Savary, B. Graff, J.-P. Fouassier, D. Gigmes, J. Toufaily, T. Hamieh, J. Lalevée, *Polym. Chem.* **2013**, *4*, 5679-5687; e) M. Caricato, C. Coluccini, D. A. Vander Griend, A. Forni, D. Pasini, *New J. Chem.* **2013**, *37*, 2792-2799; f) R. V. Pereira, M. H. Gehlen, *J. Phys. Chem. A* **2006**, *110*, 7539-7546.

[16] a) P. Flores, M. C. Rezende, F. Jara, *Dyes Pigments* **2004**, *62*, 277-281; b) S. E. Boiadjiev, D. A. Lightner, *Monatsh. Chem.* **2008**, *139*, 503-511; c) L. A. Crawford, H. McNab, *Collect. Czech. Chem. Commun.* **2009**, *74*, 995-1009; d) **S**. Wang, S.-H. Kim, *Dyes Pigments* **2009**, *80*, 314-320; e) K. Kowalski, Ł. Szczupak, J. Skiba, O. S. Abdel-Rahman, R. F. Winter, R. Czerwieniec, B. Therrien, *Organometallics* **2014**, *33*, 4697-4705.

[17] a) Y. Nagao, T. Sakai, K. Kozawa, T. Urano, *Dyes Pigments* **2007**, *73*, 344-352; b) M. C. Rezende, P. Campodonico, E. Abuin, J. Kossanyi, *Spectrochim. Acta A* **2001**, *57*, 1183-1190; c) S.-H. Kim, Y.-S. Kim, D.-H. Lee, Y.-A Son, *Mol. Cryst. Liq. Cryst.* **2011**, *550*, 240-249.

[18] a) M. A. N. Razvi, A. H. Bakry, S. M. Afzal, S. A Khan, A. M. Asiri, *Mater. Lett.* **2015**, *144*, 131-134; b) S. M. Lee, W. S. Jahng, J. H. Lee, B. K. Rhee, K. H. Park, *Chem. Phys. Lett.* **2005**, *411*, 496-500; c) J. Garín, J. Orduna, J. I. Rupérez, R. Alcalá, B. Villacampa, C. Sánchez, N. Martín, J. L. Segura, M. González, *Tetrahedron Lett.* **1998**, *39*, 3577-3580; d) R. Andreu, J. Garín, J. Orduna, R. Alcalá, B. Villacampa, *Org. Lett.* **2003**, *5*, 3143-3146; e) B. R. Cho, J. T. Je, S. J. Lee, S. H. Lee, H. S. Kim, S. J. Jeon, O.-K. Song, C. H. Wang, *J. Chem. Soc., Perkin Trans. 2* **1996**, *10*, 2141-2144; f) X. Zhou, A.-M. Ren, J.-K. Feng, X.-J. Liu, C.-C. Shu, *Chinese J. Chem.* **2004**, *22*, 38-46.

[19] M. El-Sayed, S. Spange, *J. Phys. Org. Chem.* **2007**, *20*, 264-270.

[20] a) K. Zhou, H. Fu, L. Feng, M. Cui, J. Dai, B. Liu, *Chem. Commun.* **2015**, *51*, 11665-11668; b) H. Lee, M. Y. Berezin, K. Guo, J. Kao, S. Achilefu, *Org. Lett.* **2009**, *11*, 29-32.

[21] F. Wu, L. Zhu, S. Zhao, Q. Song, C. Yang, *Dyes Pigments* **2016**, *124*, 93-100.

[22] a) S. Yagai, *J. Photoch. Photobio. C* **2006**, *7*, 164-182; b) R. B. K. Siram, K. Tandy, M. Horecha, P. Formanek, M. Stamm, S. Gevorgyan, F. C. Krebs, A. Kiriy, P. Meredith, P. L. Burn, E. B. Namdas, S. Patil, *J. Phys. Chem. C* **2011**, *115*, 14369-14376; c) R. Schmidt, M. Stolte, M. Grüne, F. Würthner, *Macromolecules* **2011**, *44*, 3766-3776.

[23] M. Klikar, F. Bureš, O. Pytela, T. Mikysek, Z. Padělková, A. Barsella, K. Dorkenoo, S. Achelle, *New. J. Chem.* **2013**, *37*, 4230-4240.

[24] M. Klikar, I. V. Kityk, D. Kulwas, T. Mikysek, O. Pytela, F. Bureš, *New J. Chem.* **2017**, DOI: 10.1039/C6NJ02994A.

[25] R. Nazir, B. Thorsted, E. Balčiunas, L. Mazur, I. Deperasińska, M. Samoć, J. Brewer, M. Farsari, D. T. Gryko, *J. Mater. Chem. C* **2016**, *4*, 167-177.

[26] a) P. Solanke, F. Bureš, O. Pytela, J. Kulhánek, Z. Padělková, *Synthesis* **2013**, *45*, 3044-3051; b) P. Solanke, F. Bureš, O. Pytela, M. Klikar, T. Mikysek, L. Mager, A. Barsella, Z. Růžičková, *Eur. J. Org. Chem.* **2015**, *24*, 5339-5349.

[27] H. Hartmann, S. Scheithauer, *J. Prakt. Chem.* **1969**, *311*, 827-843.

[28] M. Blanchard-Desce, V. Alain, P V. Bedworth, S. R. Marder, A. Fort, C. Runser, M. Barzoukas, S. Lebus, R. Wortmann, *Chem. Eur. J.* **1997**, *3*, 1091-1104.

[29] a) I. M. Downie, E. J. Martyn, H. Heaney, K. F. Shuaibar, *Tetrahedron* **1993**, *49*, 4015-4034; b) J. A. Clarke, O. Meth-Cohn, *Tetrahedron Lett.* **1975**, *52*, 4705-4708.

[30] F. Texier-Boullet, A. Foucaud, *Tetrahedron Lett.* **1982**, *23*, 4927-4928.

[31] a) C. W. Bird, *Tetrahedron* **1986**, *42*, 89-92; b) C. W. Bird, *Tetrahedron* **1985**, *41*, 1409-1414; c) S. I. Kotelevskii, O. V. Prezhdo, *Tetrahedron* **2001**, *57*, 5715-5729; d) T. M. Krygowski, H. Szatylowicz, O. A. Stasyuk, J. Dominikowska, M. Palusiak, *Chem. Rev.* **2014**, *114*, 6383-6422.

[32] A. A. Isse, A. Gennaro, *J. Phys. Chem. B* **2010**, *114*, 7894-7899.

[33] OPChem, O. Pytela, version 8.1, webpage: http://bures.upce.cz/OPgm.

[34] a) D. Cvejn, E. Michail, K. Seintis, M. Klikar, O. Pytela, T. Mikysek, N. Almonasy, M. Ludwig, V. Giannetas, M. Fakis, F. Bureš, *RSC Adv.* **2016**, *6*, 12819-12828; b) L. Yan, X. Chen, Q. He, Y. Wang, X. Wang, Q. Guo, F. Bai, A. Xia, *J. Phys. Chem. A* **2012**, *116*, 8693-8705; c) F. Terenziani, C. Le Droumaguet, C. Katan, O. Mongin, M. Blanchard-Desce, *ChemPhysChem* **2007**, *8*, 723-734.

[35] Gaussian 09, Revision D.01, M. J. Frisch, G. W. Trucks, H. B. Schlegel, G. E. Scuseria, M. A. Robb, J. R. Cheeseman, G. Scalmani, V. Barone, B. Mennucci, G. A. Petersson, H. Nakatsuji, M. Caricato, X. Li, H. P. Hratchian, A. F. Izmaylov, J. Bloino, G. Zheng, J. L. Sonnenberg, M. Hada, M. Ehara, K. Toyota, R. Fukuda, J. Hasegawa, M. Ishida, T. Nakajima, Y. Honda, O. Kitao, H. Nakai, T. Vreven, J. A. Montgomery, Jr., J. E. Peralta, F. Ogliaro, M. Bearpark, J. J. Heyd, E. Brothers, K. N. Kudin, V. N. Staroverov, T. Keith, R. Kobayashi, J. Normand, K. Raghavachari, A. Rendell, J. C. Burant, S. S. Iyengar, J. Tomasi, M. Cossi, N. Rega, J. M. Millam, M. Klene, J. E. Knox, J. B. Cross, V. Bakken, C. Adamo, J. Jaramillo, R. Gomperts, R. E. Stratmann, O. Yazyev, A. J. Austin, R. Cammi, C. Pomelli, J. W. Ochterski, R. L. Martin, K. Morokuma, V. G. Zakrzewski, G. A. Voth, P. Salvador, J. J. Dannenberg, S. Dapprich, A. D. Daniels, O. Farkas, J. B. Foresman, J. V. Ortiz, J. Cioslowski, D. J. Fox, Gaussian, Inc., Wallingford CT, **2013**.

10.1002/ejoc.201700070

WILEY-VCH

Entry for the Table of Contents

Layout 1:

Key topic: Electron Acceptor

FULL PAPER

Electron withdrawing abilities of eight popular malonic acid-derived acceptor units such as cyanoacetic acid, malonodinitrile, diethyl malonate, Meldrum´s acid, *N*,*N*´-dibutylbarbituric acid, *N*,*N*´-dibutyl-2-thiobarbituric acid, dimedone, and indan-1,3-dione have been investigated and critically compared.

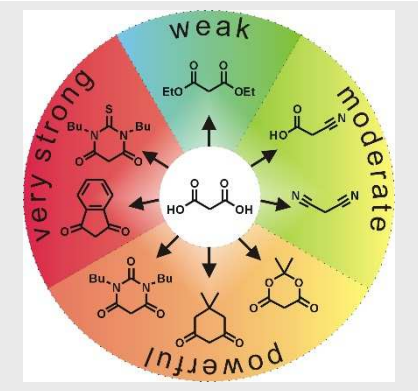

*M. Klikar, V. Jelínková, Z. Růžičková, T. Mikysek, O. Pytela, M. Ludwig, F. Bureš**

Page No. – Page No.

Malonic Acid and its Derivatives on Duty as Electron-Withdrawing Units in Push-Pull Molecules